drug-resistant viral strains and their specific mutations in a patient's clinical samples.

The guidelines for use of ARV drugs in HIV-1-infected adults and adolescents established by the US Department of Health and Human Services (DHHS) (http://www.aidsinfo.nih.gov/guidelines) recommend monitoring viral genotypic changes in patient samples and use of this information to determine which therapeutic regimens are most appropriate for the specific patient [3].

The restriction fragment mass polymorphism (RFMP) method is based on amplification and mass detection of oligonucleotides excised by type-IIS restriction enzyme digestion, using matrix-assisted laser desorption and ionization time of flight mass spectrometry (MALDI-TOF MS). RFMP-based drug-resistance testing and genotyping has been shown to be a sensitive, accurate and reliable method for clinical utility in many fields [4–12]. Especially important is that RFMP enables sensitive detection of mutations without population-based cloning and subsequent sequencing analysis [6].

In this study, we applied the RFMP assay for detection of mutations in the coding sequences for reverse transcriptase (RT) and protease (PR) of HIV-1 that engender resistance to nucleoside reverse transcriptase inhibitors (NRTIs), non-nucleoside reverse transcriptase inhibitors (NNRTIs) and protease inhibitors (PIs). Compared with direct sequencing, RFMP is shown to be a sensitive and reliable method for genotypic testing of drug-resistance mutations in HIV-1 infected patients.

## Materials and Methods

### Specimens

A total of 100 plasma samples were collected from 60 HIV-1 infected patients who had received HAART (including NRTIs, NNRTIs and PIs) at the AIDS Clinical Center, National Center for Global Health and Medicine, Japan, between 1999 and 2009. Written informed consent was obtained from each participant, and the experimental protocol conformed to the ethical guidelines of the 1975 Declaration of Helsinki, as reflected in *a priori* approval (NCGM-H22-938) by the Ethics Committee of the AIDS Clinical Center, National Center for Global Health and Medicine, Japan. The demographic characteristics are summarized in Table 1.

### HIV-1 performance panels

To assess the limit of detection ability of the RFMP assay, the HIV-1 RNA Positive Quality Control Series (ACCURUN® 315) obtained from SeraCare Life Sciences (Milford, MA, USA) was used to measure viral load in HIV-1 performance panels.

**TABLE 1. Demographic characteristics of 60 HIV-1-infected patients**

| Characteristic | Value |
|---|---|
| Mean age in years (range) | 42 (22–67) |
| No. male (%) | 53 (88) |
| No. female (%) | 7 (12) |
| Race (%) | |
| Asian | 58 (97) |
| African | 2 (3) |
| Risk factor for HIV (% of patients) | |
| Heterosexual | 14 (23) |
| Homosexual | 27 (45) |
| Haemophilia (infected blood products) | 19 (32) |
| CDC clinical stage (%) | |
| A1/A2/A3 | 0/0/0 |
| B1/B2/B3 | 17/23/13 |
| C1/C2/C3 | 5/12/20 |
| Unknown | 10 |
| Mean CD4 cell count (No. of cells/uL [range]) | 320 (12–759) |
| No. of unknown (%) | 3 (5) |
| Mean HIV-1 RNA (No. of RNA copies/mL [range]) | 43 000 (50–1 200 000) |
| No. of unknown (%) | 6 (10) |
| History of actual treatment (No. of patients) | |
| With NRTI | 2 |
| With NRTI plus NNRTI | 23 |
| With NRTI plus PI | 21 |
| With NNRTI plus PI | 1 |
| With NRTI plus NNRTI plus PI | 33 |
| With NRTI plus PI plus INI | 1 |
| With NRTI plus INI | 2 |
| With NRTI plus PI plus INI plus FI | 1 |
| With NRTI plus NNRTI plus PI plus INI plus FI | 1 |
| Interruption | 15 |

NRTI, nucleoside reverse transcriptase inhibitor; lamivudine, abacavir, emtricitabine, tenofovir, stavudine, didanosine, zidovudine; NNRTI, non-nucleoside reverse transcriptase inhibitor; efavirenz, nevirapine; PI, protease inhibitor; atazanavir, ritonavir, lopinavir, darunavir, fosamprenavir, amprenavir, nelfinavir; INI, integrase inhibitor; raltegravir; FI, fusion inhibitor; enfuvirtide.

### Construction of recombinant HIV-1 clones

Recombinant infectious HIV-1 clones with various mutations in the RT region were constructed using site-directed mutagenesis. Briefly, the mutations were introduced into the *Xma*I-*Nhe*I fragment (759 bp) of pTZNX1, which encodes Gly-15 to Ala-267 of HIV-1 RT (strain BH 10), by oligonucleotide-based mutagenesis [13]. The *Xma*I-*Nhe*I fragment was inserted into a pNL4-3-based plasmid, generating various molecular clones with the desired mutations. Each molecular clone (10 /mL as DNA) was transfected into human 293T cells ($4 \times 10^5$ cells/100-mm-diameter dish) with Fugene transfection reagent (Roche Diagnosis, Basel, Switzerland). After 48 h, culture supernatants were harvested and stored at −80°C until use. Viral loads were determined using the COBAS® Amplicor HIV-1 Monitor Test, v1.5.

### RNA extraction and cDNA amplification

HIV-1 RNA was extracted from 200 μL of plasma using the High Pure Viral RNA Kit (Roche Diagnostics, Mannheim, Germany) according to manufacturer's instructions. Purified viral RNA was dissolved in 50 μL elution buffer (nuclease-free, sterile, double distilled water). cDNA was synthesized using only the reverse transcription step component of the RNA PCR kit (TaKaRa, Otsu, Japan).

### RFMP assay

PCR reactions were performed in 25 μL reaction mixtures containing 20 mM Tris-HCl (pH 8.4), 50 mM KCl, 0.2 mM deoxynucleoside triphosphates (dNTPs), 10 pmol of primers and 0.4 U of Platinum Taq DNA polymerase (Invitrogen, Carlsbad, CA, USA). The initial denaturing phase of 5 min at 94°C was followed by a 35-cycle amplification phase containing a denaturation step at 94°C for 15 s, annealing step at 50°C for 15 s and elongation step at 72°C for 15 s, and completed with a final extension phase at 72°C for 5 min. For the RFMP analysis of codons 65, 69, 74, 103, 106, 151, 181, 184 and 215 in the HIV-1 RT region and codons 30, 46, 48, 50, 54, 82, 84 and 90 in the HIV-1 PR region, each of the forward and reverse primers contained the viral target sequence and the *Fok*I recognition sequence ggatg (Table S1). Restriction enzyme digests were performed by mixing the PCR reaction with 10 μL of buffer (50 mM potassium acetate, 20 mM Tris-acetate, 10 mM magnesium acetate and 1 mM dithiothreitol) and 1 U of *Fok*I enzyme (New England Biolabs, Beverly, MA, USA). The reaction mixtures were incubated at 37°C for 2 h. Subsequently, the digest desalting and mass analysis were performed as described previously [14].

### MALDI-TOF instrumentation and calibration

Mass spectra were acquired on a Biflex IV linear MALDI-TOF MS (Bruker Daltonics) workstation equipped with a 337 nm nitrogen laser and a nominal ion flight path length of 1.25 m. The samples were analyzed in the negative-ion mode with a total acceleration voltage of 20 kV, extraction voltage of 18.25 kV, laser attenuation of 55, and delayed extraction of long time delay mode. Typically, time-of-flight data from 20 to 50 individual laser pulses were recorded and averaged on a transient digitizer with a time base of 2 ns and delay of 24 000 ns, after which the averaged spectra were automatically converted to mass by the accompanying data-processing software. Using these settings the instrument typically provided mass accuracy of 40–80 ppm ($10^{-6}$), mass resolution of 1500–2000 and sensitivity of 10–50 fmol in the 2- to 6-kDa mass range for oligonucleotides. Oligonucleotide standards of 6mer (5′-ACGTAC-3′; 1762.2 Da) and 16mer (5′-AC GTACGTACGTACGT-3′; 4881.2 Da) with no terminal phosphate were used for mass calibration of the instrument. The presence of metal cations produces salt adducts, leading to reduced resolution and low sensitivity, so C18 reverse phase micro-column chromatography was used for desalting oligonucleotides. Non-homogeneous crystallization is obtained with the classic dried droplet preparation, and a search for a 'sweet spot' is required. Re-crystallization of sample DNAs on matrix-prespotted anchorchip plates allowed robust formation of small single crystals.

### Direct sequencing assay

To amplify the HIV-1 RT and PR regions for analysis by direct sequencing, PCR was performed with the following primers: 5′-AACAATGGCCATTGACAGAAGAAA-3′ (2614–2637 bp of HXB2), 5′-CTGTATGTCATTGACAGTCCAGCT-3′ (3299–3323 bp of HXB2) for the RT region and 5′-CTTCCCTCA GATCACTCTTTGGCAA-3′ (2248–2273 bp of HXB2), 5′-AGGGCTAATGGGAAAATTTAAAGT-3′ (2238–2561 bp of HXB2) for the PR region. PCR products were sequenced using the BigDye Terminator (version 3.1) Cycle Sequencing kit and an ABI PRISM 310 Analyzer (Applied Biosystems, Foster City, CA, USA).

### Statistics

A limit of detection test was performed by probit analysis to compare sensitivity between the RFMP and direct sequencing assays using the statistical package SAS (version 8; SAS Institute Inc., Cary, NC, USA).

## Results

### RFMP assay strategy

The RFMP assay is based on mass spectrometric analysis of small DNA fragments that include sites of mutation (Fig. S1). The first step requires PCR amplification with forward and reverse primers that introduce the *Fok*I enzyme site, ggatg (Table S1). The diagnostic fragments released by enzymatic digestion consist of various sizes from 8 nt oligomers to 14 nt oligomers for nine codons in the RT region and eight codons in the PR region, leading to facile identification of sequence variation by mass spectrum analysis. Genotypic analysis of mutations at codons 65, 69, 74, 103, 106, 151, 181, 184 and 215 in the RT region and codons 30, 46, 48, 50, 54, 54, 82, 84 and 90 in the PR region, as assessed by the RFMP assay, was determined for 100 plasma samples. The RFMP results showed distinct peaks relevant to each codon, with the mass values for each diagnostic fragment being exactly as predicted (Supplementary Material Table S2).

### Estimation of limit of detection and ability to detect mixed genotype populations

The detection limit was estimated using replicates of each of nine dilutions of HIV-1 RNA Positive Quality Control Series (ACCURUN® 315) material ranging between 10 and 5000 copies/ml. Analysis of various calibrated HIV-1 RNA dilution series determined the lower detection limit to be 223.02 copies/mL for the RFMP and 1268.11 copies/mL for the direct sequencing assays by probit analysis. The probit analysis predicts a 95% CI: 132.64–693.00 for the RFMP and 863.09–3656.80 for the direct sequencing assays (Table 2).

**TABLE 2. Limit of detection of the RFMP and direct sequencing assays**

| | | RFMP | | Direct sequencing | |
|---|---|---|---|---|---|
| HIV-1 RNA copies/ml | No. tested | No. detected | Per cent detected | No. detected | Per cent detected |
| 5000 | 10 | 10 | 100% | 10 | 100% |
| 2500 | 10 | 10 | 100% | 10 | 100% |
| 1000 | 10 | 10 | 100% | 9 | 90% |
| 500 | 10 | 10 | 100% | 4 | 40% |
| 250 | 10 | 10 | 100% | 1 | 10% |
| 100 | 10 | 8 | 80% | 0 | 0% |
| 50 | 10 | 3 | 30% | 0 | 0% |
| 25 | 10 | 1 | 10% | 0 | 0% |
| 10 | 10 | 1 | 10% | 0 | 0% |
| Limit of detection | | 223.02 copies/mL (95% CI, 132.64–693.00) | | 1268.11 copies/mL (95% CI, 863.09–3656.80) | |

Defined dilutions of HIV-1 RNA Positive Quality Control Series were made from 10 copies to 5000 copies/mL and limit of detection abilities were calculated by probit analysis at a 95% detection level.

To evaluate the ability of the RFMP assay to determine small amounts of mutant virus in mixed populations, assays were performed with recombinant HIV-1 clones composed of different ratios of wild-type (K103 in the RT region) and mutant genotypes (N103 in the RT region). Defined mixtures were prepared with the following percentages of K103N mutant virus in the total virus population: 100%, 50%, 20%, 10%, 5% and 1%. The K103N mutant virus could be detected in concentrations as low as 5% of the total virus by RFMP, whereas direct sequencing assays were able to detect mutant virus only when present in 20% or more of the total virus population (Fig. 1).

**Comparison of RFMP with direct sequencing analyses**

All 100 clinical samples from 60 patients were analysed by the RFMP and direct sequencing assays for the presence of drug resistance-related mutations: nine codons in the RT region and eight codons in the PR region of the HIV-1 *pol* gene (a total of 17 codons).

The overall concordance rates between RFMP and sequencing assays were excellent, irrespective of PR and RT regions (Table 3). Concordance rates in the RT region were 97% (97/100) at codons 65, 69, 74, 103, 151, 181 and 184, 96% (96/100) at codon 106, and 94% (94/100) at codon 215 (Fig. 2a).

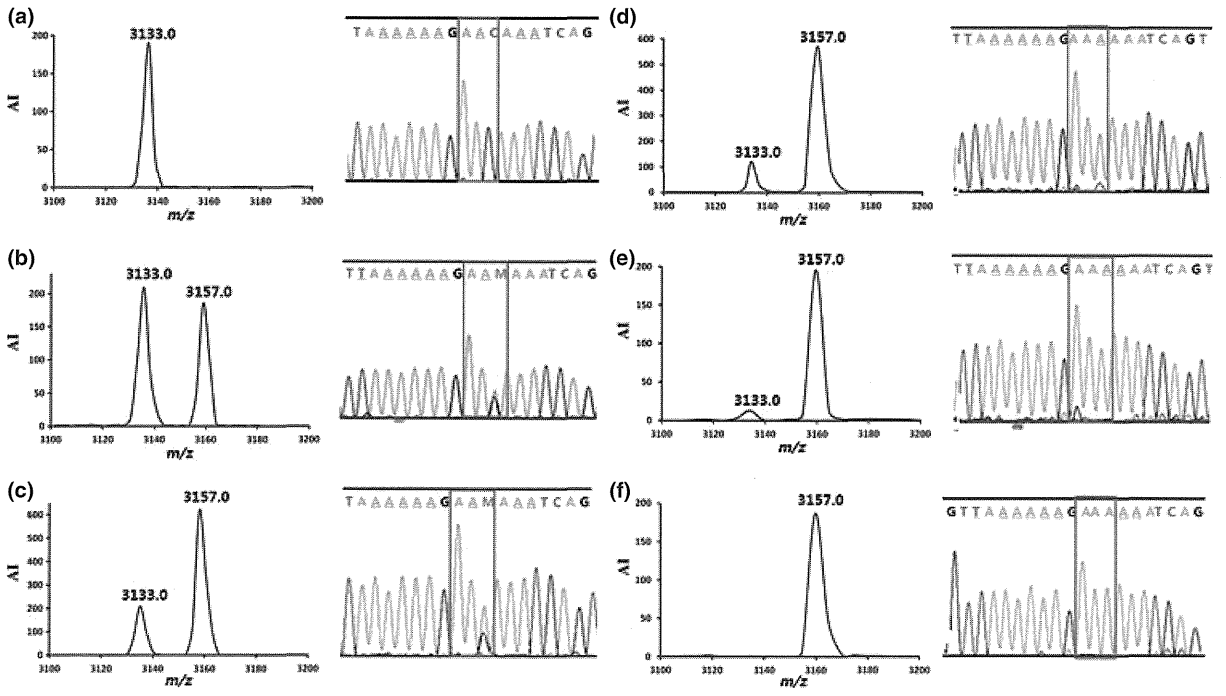


FIG. 1. Evaluation of the sensitivity of the RFMP assay for detection of minor amounts of virus with a defined mixture of K103N. The MALDI-TOF MS spectra and direct sequencing chromatograms shown are representative of experiments repeated three times using mixed populations of wild-type (K103) and NNRTI mutant (N103). The wild-type plasmids were mixed with mutant type at various ratios as follows: (a) 100%, (b) 50%, (c) 20%, (d) 10%, (e) 5% and (f) 1%. Molecular masses of 3133.0 and 3157.0 correspond to N103 and K103, respectively. AI is absolute intensity; m/z is mass-to-charge ratio.

**TABLE 3. Comparison of the results obtained by the RFMP and direct sequencing assays in 100 clinical specimens**

| *pol* gene | Codon | Discordant (*n*) | Concordant (*n*) | Compatible (*n*) | | Amino acid | |
|---|---|---|---|---|---|---|---|
| | | | | RFMP only | Direct sequencing only | RFMP | Direct sequencing |
| RT | 65 | 3 | 97 | – | – | | |
| | 69 | 3 | 97 | – | – | | |
| | 74 | 3 | 97 | – | – | | |
| | 103 | 3 | 97 | – | – | | |
| | 106 | 3 | 96 | 1 | – | V/A | V |
| | 151 | 3 | 97 | – | – | | |
| | 181 | 3 | 97 | – | – | | |
| | 184 | 3 | 97 | – | – | | |
| | 215 | 3 | 94 | 3 | – | T/F | T/F or I/S or T/I/F |
| | | | | | | T/Y | T/Y or N/S or T/S/Y |
| | | | | | | T/Y | T/Y or N/S or T/S/Y |
| PR | 30 | – | 100 | – | – | | |
| | 46 | – | 100 | – | – | | |
| | 48 | – | 100 | – | – | | |
| | 50 | – | 100 | – | – | | |
| | 54 | – | 100 | – | – | | |
| | 82 | – | 99 | 1 | – | V/A | V |
| | 84 | – | 99 | 1 | – | I/V | V |
| | 90 | – | 100 | – | – | | |

RT, reverse transcriptase; PR, protease.

Similarly, concordance rates in the PR region were 100% (100/100) at codons 30, 46, 48, 50, 54 and 90, and 99% (99/100) at codons 82 and 84 in the PR region (Fig. 2b). Both assays showed identical base substitution and amino acid composition in these positions. Rate of compatible cases were observed 1% (1/100) at codons 106, and 3% (3/100) at codon 215 in the RT region and 1% (1/100) at codons 82 and 84 in the PR region, respectively. Three samples (mixed-type) at codon 215 containing double mutations in a single codon were identified only by RFMP, as a result of the inability of the direct sequencing assay to determine the variants present in the clinical samples. As shown in Fig 2(c), 215T/Y mixtures detected by RFMP could be scored as 215T (ACC) plus 215Y (TAC), or 215N (AAC) plus 215S (TCC), or 215T (ACC) plus 215S (TCC) plus 215Y (TAC), by direct sequencing. A compatible single nucleotide mixture at one position was observed in three samples at three codons (codon 106 in the RT; codon 82, 84 in the PR), respectively. Of these, the RFMP assay detected more mixed samples than the direct sequencing assay. The details of mixtures detected by both assays are shown in Table 3. Discordances between the two assays occurred for three samples at RT region codons, which had undetectable viral loads; the correct viral genotypes were identified only by RFMP assay.

## Discussion

ARV drug-resistance is a major obstacle in the effective clinical management of HIV-1-infected patients [3,15] and therapeutic strategies must maximize the early detection of drug resistance mutations. Having a sensitive genotyping assay that can detect with high accuracy and reliability, drug-resistance mutations that emerge during HAART can be very important for the optimization of ARV regimens, improvement of patient treatment and outcome of therapy. The RFMP assay has been demonstrated to be a sensitive, accurate and reliable method for genotyping and detecting drug-resistance mutations in several viruses, including hepatitis and papillomavirus [4,6,8–12].

In the present study, we validated use of the MALDI-TOF MS-based RFMP assay to detect oligonucleotides containing 8–14 nucleotides for codons implicated with ARV drug-resistance mutations. Specifically, we established successful detection at codons 65, 69, 74, 103, 106, 151, 181, 184 and 215 in the HIV-1 RT coding region, and 30, 46, 48, 50, 54, 82, 84 and 90 in the HIV-1 PR coding region. These codons address resistance to all approved NRTI and NNRTI inhibitors [16–18]: mutation at RT codon 65 (K65R) confers resistance to tenofovir, didanosine and abacavir; RT mutation L74V confers resistance to didanosine and abacavir; the K103N RT mutation engenders resistance to the NNRTIs efavirenz and nevirapine; the Q151M RT mutation causes resistance to AZT, D4T, didenosine and abacavir through the decreased incorporation mechanism; Y181C causes resistance to nevirapine, etravirine and rilpivirine; M184V/I confers resistance to 3TC and FTC, and also affects resistance to rilpivirine; and finally, T215Y causes resistance to AZT and D4T through the excision mechanism. In addition, mutations at the 30, 46, 48, 50, 54, 82, 84 and 90 sites of the HIV-1 PR coding region cause resistance to all known protease inhibitors: specifically, D30N causes resistance to nelfinavir; M46I/L causes resistance to nelfinavir and indinavir; G48V/M causes resistance to atazanavir, nelfinavir and saquinavir; I50L/V causes resistance to atazanavir, darunavir, fosamprenavir and lopinavir; and mutations at

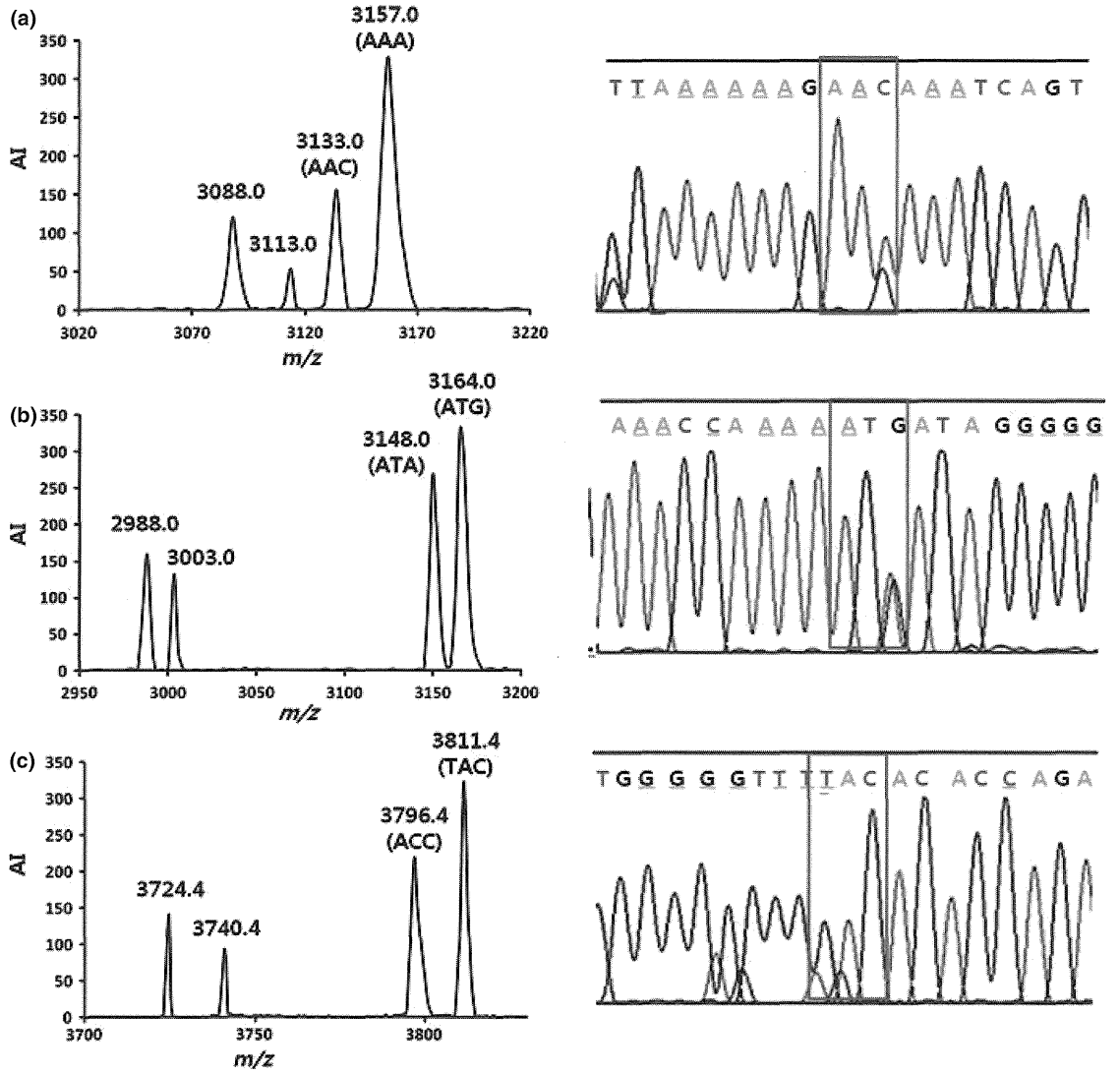


FIG. 2. Comparison of the RFMP and direct sequencing assays for detection of mixed genotypes. Sera were taken from patients infected with HIV-1 carrying ARV drug-resistant mutations and examined by the RFMP and sequencing assays. (a) For codon 103, molecular masses of 3088.0/3157.0 and 3113.0/3133.0 represent Lys (AAA) and Asn (AAC), respectively. (b) For codon 46, molecular masses of 2988.0/3164.0 and 3003.0/3148.0 represent Met (ATG) and Ile (ATA), respectively. (c) For codon 215, molecular masses of 3740.4/3796.4 and 3724.4/3811.4 represent Thr (ACC) and Tyr (TAC), respectively. Each codon was indicated by a red box in the sequencing chromatogram. AI is absolute intensity; m/z is mass-to-charge ratio.

residues 54, 82, 84 and 90 cause resistance to all protease inhibitors to a varying extent (http://hivdb.stanford.edu/DR/PIResiNote.html).

The detection limit of the RFMP assay was determined to be 223.02 copies/mL and able to identify a minority mutant at a concentration as low as 5% of the circulating mixed populations, whereas the detection limit of the direct sequencing method was 1268.11 copies/mL and able to detect variants only when present at >20% of the total population (Table 2 and Fig. 1). A clear correlation was observed between peak ratios and relative genotype concentration of mixed populations.

The performance of the RFMP assay in detecting mutations related to ARV drug-resistance was compared with direct sequencing assays for 100 clinical samples from 60 HIV-1-infected patients who experienced HAART therapy. The RFMP assay successfully identified genotypic changes at all 17 codons tested in clinical samples. Compared with direct sequencing, the RFMP assay exhibited 96.6% concordance in the RT region and 99.8% concordance in the PR region (Table 3 and Fig 2). The PR data were not significantly more concordant than the RT data (the difference was only two cases). The reason for the slight difference is not clear, thus further investigation is required with more samples. Notably, the RFMP assay

outperformed direct sequencing for the detection of single and double mutations in compatible samples. The RFMP assay detected 1% (1/100) more mutant viruses in codons 106, 82 and 84 and 3% (3/100) more mutant viruses in codon 215. All discordances between the two assays were due to the inability of the direct sequencing assay to identify the residues at nine RT codons in three patients. Hence, the discrepancy among the two assays may be due to a lower sensitivity of direct sequencing.

HAART can clearly extend the life expectancy of HIV-1 patients. However, as adherence is usually imperfect, continuous ARV drug-resistance testing can be an important management tool. There are two major methods of assessing ARV drug-resistance: phenotypic assays and genotypic assays that provide complementary information and be preferable to the other [19,20]. Current treatment guidelines define as treatment failure the detection of more than 200 copies/mL of HIV-1 RNA [3]. However, existing genotypic assays, such as direct sequencing and the reverse hybridization-based assay, do not reliably detect fewer than 1000 copies/ml of HIV-1 RNA, nor do they enable detection of sequence variants present at <20% of minority variants in mixed populations [21,22]. This performance does not allow facile interpretation of ratios between multiple virus mixtures, especially when a double mutation is present in a single codon. While the reverse hybridization-based assay has somewhat higher sensitivity than direct sequencing it gives rise to false-positive and false-negative results more frequently than direct sequencing [21–26].

With the advent of Next Generation Sequencing methods it is possible to detect, by 454 pyrosequencing or an Illumina Genome Analyzer, minor viral variants whose prevalence is <1%. 454 pyrosequencing, also called ultra-deep pyrosequencing (UDPS), relies on fixing nebulized and adapter-ligated DNA fragments to small DNA-capture beads in a water-in-oil emulsion. The DNA fixed to these beads is then amplified by PCR. An advantage of UDPS in the case of viral genomic analysis is that it yields long sequence information for each sample (average ~800 bases). However, UDPS has some technical challenges. A major limitation of the UDPS relates to resolution of homopolymer-containing DNA segments, such as AAA and GGG [27]. Because there is no terminating moiety preventing multiple consecutive incorporations at a given cycle, pyrosequencing relies on the magnitude of light emitted to determine the number of repetitive bases. This is prone to greater error than misincorporation. Hence, the dominant error type for the 454 platform is insertion-deletion, rather than substitution. The decrease in single read accuracy from 99.4% for test fragments to 96% for genomic libraries is primarily due to a lack of clonality in a fraction of the genomic templates in the emulsion [28]. Moreover, based on current list prices for the UDPS, the current cost for all the reagents, including the picotiter plate, library preparation kits and emulsion PCR kits, to perform a single experiment is $1000–7000 [29].

By combining the merits of unique assay chemistry and the mature nature of MALDI-TOF mass spectrometry, the RFMP assay can be used to screen for HIV drug-resistance mutations in a robust high-throughput manner (e.g. 96 samples can be analysed in 3 h with Bruker software (flexcontrol 3.0), which is faster than existing hybridization or sequencing-based methods). In terms of cost-effectiveness, the direct cost per test (reagents and labour) of the RFMP assay can be <$30, including viral DNA extraction, PCR, restriction digestion, desalting and matrix for mass analysis, which is cheaper than the sequencing or hybridization assays that are c. $50–100 per test. These costs do not include the equipment costs, which are slightly greater for the RFMP method. However, with the advent of many diagnostic assays operating on a mass spectrometer platform, such as clinical genotyping and microorganism identification, and the gradual spread of compact mass spectrometers into laboratories as medical devices (i.e. Bruker Microflex), the burden of the amortization cost should be substantially reduced [30]. A limitation of the RFMP assay is that it determines only molecular mass and is thus applicable only to known resistance mutations and may fail to detect DNA sequence changes that do not affect molecular mass. Moreover, the occurrence of a novel resistance mutation with sequence alterations that cause a deviation from the predicted molecular mass pattern should be addressed by periodic updating of mass patterns for unambiguous result interpretation from up-to-date HIV databases.

We demonstrate here that the mass spectrometry-based RFMP assay is highly sensitive and able to successfully detect HIV-1 carrying drug-resistant mutations that are present in <5% of the total virus population. Hence, this assay can be used for the efficient assessment of genotype dynamics of viral quasispecies. Therefore, this simple procedure can be easily adapted to a high-throughput format, should enable earlier detection of drug-resistant viruses and help elucidate mechanisms of HIV-1 resistance, as well as guide and optimize treatment decisions.

## Acknowledgements

We thank Doctors Yukiko Takahashi and Fujie Negishi for clinical sample preparation.

## Transparency Declaration

This work was supported by grants from the Ministry of Knowledge and Economy, Bilateral International Collaborative

R&D Program, Republic of Korea, and in part by NIH grants AI076119, AI094715, AI074389, AI073975 and AI077424.

## Supporting Information

Additional Supporting Information may be found in the online version of this article:

**Figure S1.** Schematic representation of the RFMP strategy.

**Table S1.** Primers used in PCR amplification for the RFMP assay.

**Table S2.** Expected masses of oligonucleotides resulting from restriction enzyme digestion of PCR products.

## References


1. Chen TK, Aldrovandi GM. Review of hiv antiretroviral drug resistance. *Pediatr Infect Dis J* 2008; 27: 749–752.
2. Boltz VF, Zheng Y, Lockman S *et al.* Role of low-frequency hiv-1 variants in failure of nevirapine-containing antiviral therapy in women previously exposed to single-dose nevirapine. *Proc Natl Acad Sci USA* 2011; 108: 9202–9207.
3. Thompson MA, Aberg JA, Hoy JF *et al.* Antiretroviral treatment of adult hiv infection: 2012 recommendations of the international antiviral society-USA panel. *JAMA* 2012; 308: 387–402.
4. Hong SP, Shin SK, Lee EH *et al.* High-resolution human papillomavirus genotyping by maldi-tof mass spectrometry. *Nat Protoc* 2008; 3: 1476–1484.
5. Oh HB, Kim SO, Cha CH *et al.* Identification of hepatitis c virus genotype 6 in korean patients by analysis of 5' untranslated region using a matrix assisted laser desorption/ionization time of flight-based assay, restriction fragment mass polymorphism. *J Med Virol* 2008; 80: 1712–1719.
6. Cha CK, Kwon HC, Cheong JY *et al.* Association of lamivudine-resistant mutational patterns with the antiviral effect of adefovir in patients with chronic hepatitis b. *J Med Virol* 2009; 81: 417–424.
7. Cha YS, Choi SH, Lee JH *et al.* Analysis of tpox short tandem repeat locus with matrix-associated laser desorption/ionization time-of-flight-based restriction fragment mass polymorphism assay. *Anal Biochem* 2011; 412: 79–84.
8. Cho SW, Koh KH, Cheong JY *et al.* Low efficacy of entecavir therapy in adefovir-refractory hepatitis b patients with prior lamivudine resistance. *J Viral Hepatitis* 2010; 17: 171–177.
9. Choe WH, Hong SP, Kim BK *et al.* Evolution of hepatitis b virus mutation during entecavir rescue therapy in patients with antiviral resistance to lamivudine and adefovir. *Antivir Ther* 2009; 14: 985–993.
10. Han KH, Hong SP, Choi SH *et al.* Comparison of multiplex restriction fragment mass polymorphism and sequencing analyses for detecting entecavir resistance in chronic hepatitis b. *Antivir Ther* 2011; 16: 77–87.
11. Kim SS, Cheong JY, Lee D *et al.* Adefovir-based combination therapy with entecavir or lamivudine for patients with entecavir-refractory chronic hepatitis b. *J Med Virol* 2012; 84: 18–25.
12. Lee JM, Kim HJ, Park JY *et al.* Rescue monotherapy in lamivudine-resistant hepatitis b e antigen-positive chronic hepatitis b: Adefovir versus entecavir. *Antivir Ther* 2009; 14: 705–712.
13. Kodama EI, Kohgo S, Kitano K *et al.* 4'-ethynyl nucleoside analogs: potent inhibitors of multidrug-resistant human immunodeficiency virus variants in vitro. *Antimicrob Agents Chemother* 2001; 45: 1539–1546.
14. Kim HS, Han KH, Ahn SH *et al.* Evaluation of methods for monitoring drug resistance in chronic hepatitis b patients during lamivudine therapy based on mass spectrometry and reverse hybridization. *Antivir Ther* 2005; 10: 441–449.
15. Tsibris AM, Hirsch MS. Antiretroviral therapy in the clinic. *J Virol* 2010; 84: 5458–5464.
16. Singh K, Marchand B, Kirby KA, Michailidis E, Sarafianos SG. Structural aspects of drug resistance and inhibition of hiv-1 reverse transcriptase. *Viruses* 2010; 2: 606–638.
17. Sarafianos SG, Marchand B, Das K *et al.* Structure and function of hiv-1 reverse transcriptase: molecular mechanisms of polymerization and inhibition. *J Mol Biol* 2009; 385: 693–713.
18. Tang MW, Shafer RW. Hiv-1 antiretroviral resistance: scientific principles and clinical applications. *Drugs* 2012; 72: e1–e25.
19. Underwood MR, Ross LL, Irlbeck DM *et al.* Sensitivity of phenotypic susceptibility analyses for nonthymidine nucleoside analogues conferred by k65r or m184v in mixtures with wild-type hiv-1. *J Infect Dis* 2009; 199: 84–88.
20. Qari SH, Winters M, Vandamme AM, Merigan T, Heneine W. A rapid phenotypic assay for detecting multiple nucleoside analogue reverse transcriptase inhibitor-resistant hiv-1 in plasma. *Antivir Ther* 2002; 7: 131–139.
21. Sen S, Tripathy SP, Paranjape RS. Antiretroviral drug resistance testing. *J Postgrad Med* 2006; 52: 187–193.
22. Garcia-Gonzalez C, Garcia-Bujalance S, Ruiz-Carrascoso G *et al.* Detection and quantification of the k103n mutation in hiv reverse transcriptase by pyrosequencing. *Diagn Microbiol Infect Dis* 2012; 72: 90–96.
23. Clevenbergh P, Durant J, Halfon P *et al.* Persisting long-term benefit of genotype-guided treatment for hiv-infected patients failing haart. The viradapt study: week 48 follow-up. *Antivir Ther* 2000; 5: 65–70.
24. Cortez KJ, Maldarelli F. Clinical management of hiv drug resistance. *Viruses* 2011; 3: 347–378.
25. Erali M, Page S, Reimer LG, Hillyard DR. Human immunodeficiency virus type 1 drug resistance testing: a comparison of three sequence-based methods. *J Clin Microbiol* 2001; 39: 2157–2165.
26. Garcia-Bujalance S, de Guevara CL, Gonzalez-Garcia J, Arribas JR, Gutierrez A. Comparison between sequence analysis and a line probe assay for testing genotypic resistance of human immunodeficiency virus type 1 to antiretroviral drugs. *J Clin Microbiol* 2005; 43: 4186–4188.
27. Rothberg JM, Leamon JH. The development and impact of 454 sequencing. *Nat Biotechnol* 2008; 26: 1117–1124.
28. Margulies M, Egholm M, Altman WE *et al.* Genome sequencing in microfabricated high-density picolitre reactors. *Nature* 2005; 437: 376–380.
29. Hert DG, Fredlake CP, Barron AE. Advantages and limitations of next-generation sequencing technologies: a comparison of electrophoresis and non-electrophoresis methods. *Electrophoresis* 2008; 29: 4618–4626.
30. Nagy E, Maier T, Urban E, Terhes G, Kostrzewa M. Species identification of clinical isolates of bacteroides by matrix-assisted laser-desorption/ionization time-of-flight mass spectrometry. *Clin Microbiol Infect* 2009; 15: 796–802.

J Infect Chemother (2013) 19:850–857
DOI 10.1007/s10156-013-0576-y

ORIGINAL ARTICLE

# Urinary beta-2 microglobulin and alpha-1 microglobulin are useful screening markers for tenofovir-induced kidney tubulopathy in patients with HIV-1 infection: a diagnostic accuracy study

**Takeshi Nishijima · Takuro Shimbo · Hirokazu Komatsu · Misao Takano · Junko Tanuma · Kunihisa Tsukada · Katsuji Teruya · Hiroyuki Gatanaga · Yoshimi Kikuchi · Shinichi Oka**

Received: 26 November 2012 / Accepted: 14 February 2013 / Published online: 7 March 2013


**Abstract** Kidney tubulopathy is a well-known adverse event of antiretroviral agent tenofovir. A cross-sectional study was conducted to compare the diagnostic accuracy of five tubular markers, with a collection of abnormalities in these markers as the reference standard. The study subjects were patients with HIV-1 infection on ritonavir-boosted darunavir plus tenofovir/emtricitabine with suppressed viral load. Kidney tubular dysfunction (KTD) was predefined as the presence of at least three abnormalities in the following five parameters: β2-microglobulinuria (β2M), α1-microglobulinuria (α1M), high urinary *N*-acetyl-β-D-glucosaminidase (NAG), fractional excretion of phosphate ($FE_{IP}$), and fractional excretion of uric acid ($FE_{UA}$). Receiver operating characteristic curves and areas under the curves (AUC) were estimated, and the differences between the largest AUC and each of the other AUCs were tested using a nonparametric method. The cutoff value of each tubular marker was determined using raw data of 100 % sensitivity with maximal specificity. KTD was diagnosed in 19 of the 190 (10 %) patients. The AUCs (95 % CIs) of each tubular marker were β2M, 0.970 (0.947–0.992); α1M, 0.968 (0.944–0.992); NAG, 0.901 (0.828–0.974); $FE_{IP}$, 0.757 (0.607–0.907), and $FE_{UA}$, 0.762 (0.653–0.872). The AUCs of β2M and α1M were not significantly different, whereas those of the other three markers were smaller. The optimal cutoff values with 100 % sensitivity were 1,123 μg/gCr (β2M, specificity 89 %), 15.4 mg/gCr (α1M, specificity 87 %), 3.58 U/gCr (NAG, specificity 46 %), 1.02 % ($FE_{IP}$, specificity 0 %), and 3.92 % ($FE_{UA}$, specificity 12 %). Urinary β2M and α1M are potentially suitable screening tools for tenofovir-induced KTD. Monitoring either urinary β2M or α1M should be useful in early detection of tenofovir nephrotoxicity.

**Keywords** Tenofovir · Kidney tubular dysfunction · Screening · Urinary beta-2 microglobulin · Urinary alpha-1 microglobulin · HIV-1 infection

T. Nishijima · M. Takano · J. Tanuma · K. Tsukada · K. Teruya · H. Gatanaga (✉) · Y. Kikuchi · S. Oka
*AIDS Clinical Center, National Center for Global Health and Medicine, 1-21-1, Toyama, Shinjuku, Tokyo 162-0052, Japan*
e-mail: higatana@acc.ncgm.go.jp

T. Nishijima · H. Gatanaga · S. Oka
Center for AIDS Research, Kumamoto University, Kumamoto, Japan

T. Shimbo
Department of Clinical Research and Informatics, International Clinical Research Center, National Center for Global Health and Medicine, 1-21-1, Toyama, Shinjuku, Tokyo, Japan

H. Komatsu
Department of Community Care, Saku Central Hospital, Nagano, Japan

## Introduction

Tenofovir disoproxil fumarate (TDF), a prodrug of tenofovir, is a widely used nucleotide reverse transcriptase inhibitor (NRTI) as part of the initial antiretroviral therapy for patients with human immunodeficiency (HIV) infection, as well as in treatment of hepatitis B virus infection [1–4]. Tenofovir is excreted through the kidney by glomerular filtration and active tubular secretion. Renal proximal tubular damage is a well-known adverse effect of tenofovir, which sometimes leads to diabetes insipidus, Fanconi syndrome, and acute renal failure [5–7], and patients on TDF are more likely to develop renal dysfunction than those on other NRTIs [8, 9]. Of note, low

bone mineral density, another adverse effect of TDF, sometimes occurs as a result of kidney proximal tubulopathy associated with phosphate wasting and increased bone turnover [10, 11].

The risk of clinically relevant tenofovir-induced nephrotoxicity is considered to be relatively low [9, 12, 13]. However, tenofovir renal safety has not been confirmed in the long term. Importantly, both HIV infection and hepatitis B infection require long-term treatment, especially for HIV infection, where the treatment is lifelong. In tenofovir-induced nephrotoxicity, tubular dysfunction usually precedes the decline in glomerular filtration rate (GFR), suggesting that tubular markers are more sensitive than estimated GFR (eGFR) calculated with serum creatinine in screening for tenofovir nephrotoxicity [9, 14–16]. Thus, it is important to identify a renal tubular marker with high sensitivity to screen for tenofovir-induced KTD.

There is no gold standard for the diagnosis of tenofovir-induced kidney tubular dysfunction (KTD). Previous reports usually applied a collection of abnormalities in tubular function parameters as diagnostic criteria [17, 18]. However, the criteria used in each study differ, and it is often cumbersome and costly to monitor multiple renal tubular markers in practice. To our knowledge, there are no studies that have compared the diagnostic accuracy of various tubular markers for tenofovir-induced KTD. Furthermore, several pathological conditions are associated with KTD, such as active infection, diabetic nephropathy, and preexisting renal impairment [19, 20], making it difficult to evaluate KTD induced exclusively by tenofovir.

Based on the foregoing background, we designed the present study to identify the best screening marker(s) of tubular dysfunction in tenofovir-induced KTD, using a collection of abnormalities in kidney tubular markers as the reference standard.

## Patients and methods

### Ethics statement

This study was approved by the Human Research Ethics Committee of the National Center for Global Health and Medicine, Tokyo, Japan. Each patient in this study provided a written informed consent for publication of clinical data for research purpose. The study was conducted according to the principles expressed in the Declaration of Helsinki.

### Study design

This study was designed and reported according to the recommendations of the standards for reporting of diagnostic accuracy (STARD) statement [21]. We performed a single-center cross-sectional study to compare the diagnostic accuracies of various kidney tubular markers for tenofovir-induced KTD, with a collection of abnormalities in these markers as the reference standard, to identify the best screening marker in tenofovir-treated Japanese patients with HIV infection.

### Study subjects

The study population has been previously reported [22]. The study enrolled consecutive Japanese patients with HIV infection, aged >17 years, with HIV-1 viral load <200 copies/ml, and on at least 4-week treatment with once-daily ritonavir (100 mg)-boosted darunavir (800 mg) plus fixed-dose tenofovir (300 mg)/emtricitabine (200 mg), seen at our clinic between October 1, 2011 and March 31, 2012. The exclusion criteria were (1) active infection, (2) malignancy, (3) diabetes mellitus, defined by the use of glucose-lowering agents or fasting plasma glucose >126 mg/dl or plasma glucose >200 mg/dl on two different days, (4) alanine aminotransferase 2.5 times more than the upper limit of normal, (5) estimated glomerular filtration rate (eGFR) calculated by Cockcroft–Gault equation of <50 ml/min [creatinine clearance = [(140 − age) × weight (kg)]/(serum creatinine × 72)(×0.85 for females)] [23], and (6) patients who did not sign the consent form.

### Measurements

Blood and spot urine samples were collected on the same day (either on the day of enrollment or on the next visit), together with body weight measurement. The blood samples were used to measure serum creatinine, serum uric acid, serum phosphate, CD4 count, and C-reactive protein (CRP); urine samples were used to measure phosphate, uric acid, creatinine, β2-microglobulin (β2M), α1-microglobulin (α1M), and *N*-acetyl-β-D-glucosaminidase (NAG). The values of β2M, α1M, and NAG measured in the urine samples were expressed relative to urinary creatinine of 1 gl/l (/g Cr) [24].

Urinary concentrations of β2M and α1M were measured with a latex aggregation assay kit (β2M, BMG-Latex X1 "Seiken"; Denka Seiken, Niigata, Japan; α1M, Eiken α1M-III; Eiken Chemical, Tokyo, Japan), and those of NAG by colorimetric assay of enzyme activity with 6-methyl-2-pyridyl-*N*-acetyl-1-thio-β-D-glucosaminide as substrate (Nittobo Medical, Tokyo, Japan).

### Definition of renal proximal tubular dysfunction

KTD was predefined as the presence of at least three abnormalities in the following five parameters: fractional excretion of phosphate ($FE_{IP}$) {[(urine phosphate × serum creatinine)/(serum phosphate × urine creatinine)] × 100} > 18 %,

fractional excretion of uric acid ($FE_{UA}$) {[(urine uric acid × serum creatinine)/(serum uric acid × urine creatinine)] × 100)} > 15 %, β2-microglobulinuria (β2M > 1,000 μg/g Cr), α1-microglobulinuria (α1M > 16.6 mg/g Cr), and high NAG level in urine (NAG > 5.93 U/g Cr). The definition of KTD and the foregoing cutoff levels were determined based on the published reports [18, 25, 26].

The potential risk factors for KTD were determined according to previous studies and collected together with the basic demographics from the medical records [14, 27–30]: included were age, sex, body weight, and presence or absence of other medical conditions (concurrent use of other nephrotoxic drugs such as ganciclovir, sulfamethoxazole/trimethoprim, and nonsteroidal antiinflammatory agents; coinfection with hepatitis B, defined by positive hepatitis B surface antigen; coinfection with hepatitis C, defined by positive HCV viral load; hypertension, defined by current treatment with antihypertensive agents or two successive measurements of systolic blood pressure >140 mmHg or diastolic blood pressure >90 mmHg in the clinic; dyslipidemia, defined by current treatment with lipid-lowering agents or two successive measurements of either low density lipoprotein cholesterol >140 mg/dl, high density lipoprotein cholesterol <40 mg/dl, total cholesterol >240 mg/dl, triglyceride >500 mg/dl). At our clinic, blood pressure and body weight are measured every visit. We used the data on or closest to and preceding the day of blood/urine sample collection by no more than 180 days.

### Statistical analysis

The baseline characteristics of patients with KTD and those without tubular dysfunction were compared by the Student's *t* test for continuous variables (e.g., kidney tubular markers), and by the $\chi^2$ test or Fisher's exact test for categorical variables. Box plots were constructed for tubular markers of KTD and non-KTD. Diagnostic test comparison was performed using KTD as the dichotomous variable. Receiver operating characteristic (ROC) curves were constructed for individual markers, and the area under the curve (AUC) was estimated with 95 % confidence interval. The differences between the largest AUC and each of the other AUCs were tested using a nonparametric method [31], and multiple comparisons were adjusted with the Bonferroni correction. The cutoff value for each tubular marker was determined using raw data of 100 % sensitivity with maximal specificity because this point would diagnose all KTD cases with minimal false positives. For reference, two methods commonly applied for the identification of optimal cutoff points using the ROC curve were also applied: method 1 [the point on the curve closest to the point with sensitivity of one and one minus specificity of zero, calculated as the minimal value for $(1-\text{sensitivity})^2 + (1-\text{specificity})^2$]; and method 2 [the maximum vertical distance between the ROC curve and the diagonal line, calculated as the maximum value for (sensitivity + specificity − 1)] [32]. A $p$ value <0.05 was considered statistically significant. Nonparametric methods to compare AUC of tubular makers were performed with Stata software SE ver. 12 (College Station, TX, USA). All other statistical analyses were performed with the Statistical Package for Social Sciences ver. 17.0 (SPSS, Chicago, IL, USA).

## Results

A total of 190 patients were enrolled from whom blood and urine samples available for analysis (Fig. 1). Among them, 19 patients (10 %) fulfilled the criteria for KTD. The baseline characteristics and laboratory data for patients

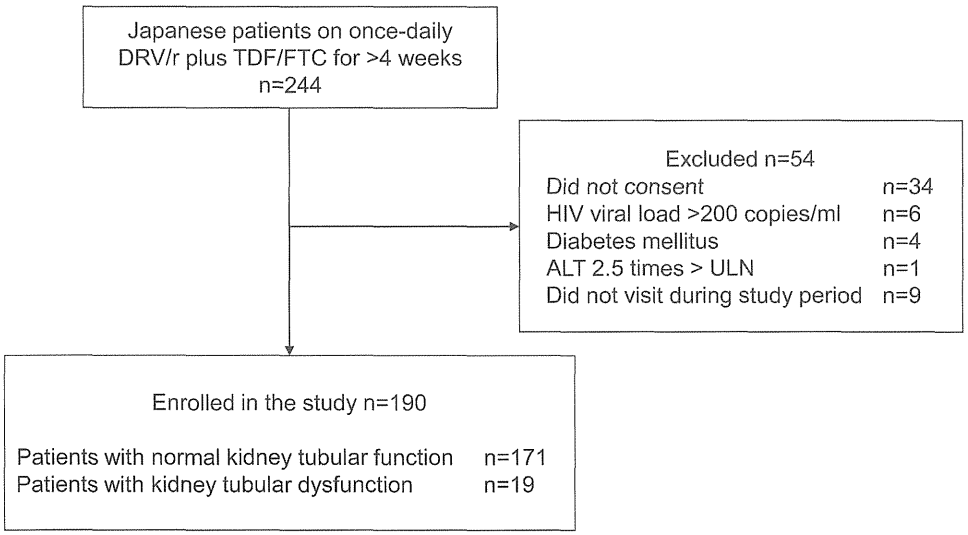


**Fig. 1** Patient enrollment. *DRV/r* ritonavir-boosted darunavir; *TDF/FTC* tenofovir/emtricitabine; *ALT* alanine transaminase; *ULN* upper limit of normal

with KTD and patients without tubular dysfunction are listed in Table 1. Patients with KTD were older ($p < 0.001$), had a lower body weight ($p = 0.006$) and lower eGFR ($p = 0.003$), and were more likely to be hypertensive than patients with normal tubular function, although the difference was not significant ($p = 0.088$). The median duration of tenofovir therapy was 71.5 weeks [interquartile range (IQR), 36.8–109.2 weeks] for the entire study population and was not different between the two groups ($p = 0.888$).

Differences in tubular markers between patients with KTD and those without KTD are shown in Table 1 and box-and-whisker plots in Fig. 2. Patients with KTD had higher levels of all five tubular markers with $p$ value <0.001 (Fig. 2). The performance of each tubular marker in differentiating patients with KTD from those with normal tubular function is illustrated by ROC curves (Fig. 3a). The AUCs and 95 % confidence intervals for the diagnosis of KTD by each tubular marker were β2M, 0.970 (0.947–0.992); α1M, 0.968 (0.944–0.992); NAG, 0.901 (0.828–0.974); $FE_{IP}$, 0.757 (0.607–0.907); and $FE_{UA}$, 0.762 (0.653–0.872). Results of comparisons of AUCs of β2M (with the largest AUC) and other markers are shown in Fig. 3b. The AUCs of β2M and α1M were not significantly different, whereas the AUCs of both $FE_{IP}$ and $FE_{UA}$ were significantly smaller than that of β2M. The AUC of NAG was marginally smaller than that of β2M with a single test, but the difference was no longer significant after adjustment of Bonferroni correction (Fig. 3b). Thus, urinary β2M and α1M had the best diagnostic performances for detecting KTD.

## Identifying optimal cutoff point for tubular markers

The cutoff values for the different tubular markers with 100 % sensitivity and the maximal specificity were as follows: β2M, 1,123.2 μg/g Cr (specificity, 89 %); α1M, 15.4 mg/g Cr (specificity, 87 %); NAG, 3.58 U/g Cr (specificity, 46 %); $FE_{IP}$, 1.02 % (specificity, 0 %); and $FE_{UA}$, 3.92 % (specificity, 12 %) (Table 2). The cutoff values determined by the aforementioned two conventional methods are also listed in Table 2. The cutoff values of both β2M and α1M by method 1 yielded the high diagnostic accuracy (β2M, 1,612 μg/g Cr, sensitivity 95 %, specificity 93 %; α1M, 16.5 mg/g Cr, sensitivity 95 %, specificity 90 %), whereas the cutoff values for these two markers calculated with method 2 were the same as the aforementioned ones with 100 % sensitivity and maximal specificity. Methods 1 and 2 yielded the same cutoff value for NAG of 5.96 U/g Cr (sensitivity 90 %, specificity 86 %). For $FE_{IP}$ and $FE_{UA}$, the sensitivity was relatively low with the cutoffs gained with method 1 and method 2, suggesting that $FE_{IP}$ and $FE_{UA}$ are not useful for screening KTD (Table 2).

**Table 1** Characteristics of patients with and without kidney tubular dysfunction (KTD)

| | KTD ($n = 19$) | Non-KTD ($n = 171$) | $p$ value |
|---|---|---|---|
| Kidney tubular markers | | | |
| β2M > 1,000 μg/g Cr, *n* (%) | 19 (100) | 21 (12.3) | <0.001 |
| α1M > 16.6 mg/g Cr, *n* (%) | 18 (94.7) | 17 (9.9) | <0.001 |
| NAG > 5.93 U/g Cr, *n* (%) | 17 (89.5) | 23 (13.5) | <0.001 |
| Fractional excretion of phosphate >18 %, *n* (%) | 5 (26.3) | 2 (1.2) | <0.001 |
| Fractional excretion of uric acid >15 %, *n* (%) | 2 (10.5) | 4 (2.3) | 0.112 |
| Characteristics | | | |
| Sex (male), *n* (%) | 18 (94.7) | 166 (97.1) | 0.473 |
| Age (years)[a] | 60 (41–62) | 38 (32–42) | <0.001 |
| Route of transmission (homosexual contact), *n* (%) | 16 (84.2) | 153 (89.5) | 0.528 |
| Weight (kg)[a] | 56 (53.5–66.5) | 67.2 (58.1–75) | 0.006 |
| eGFR (ml/min/1.73 $m^2$)[a] | 75.5 (62.8–93.5) | 87.7 (77.5–98) | 0.003 |
| Serum creatinine (mg/dl)[a] | 0.85 (0.68–0.96) | 0.80 (0.73–0.88) | 0.168 |
| CD4 cell count (/μl)[a] | 380 (194–501) | 379 (275–533) | 0.261 |
| Serum phosphate (mg/dl)[a] | 3.4 (2.7–3.7) | 3.2 (2.9–3.6) | 0.815 |
| Serum uric acid (mg/dl)[a] | 4.7 (4.2–5.7) | 5.6 (4.8–6.4) | 0.080 |
| Nephrotoxic drugs, *n* (%) | 2 (10.5) | 12 (7.0) | 0.420 |
| Hepatitis C, *n* (%) | 0 (0) | 3 (1.8) | 0.728 |
| Hepatitis B, *n* (%) | 2 (10.5) | 24 (14) | 0.501 |
| Dyslipidemia, *n* (%) | 4 (21.1) | 54 (31.6) | 0.253 |
| Hypertension, *n* (%) | 8 (42.1) | 42 (24.6) | 0.088 |
| C-reactive protein (mg/dl)[a] | 0.07 (0.03–0.28) | 0.07 (0.03–0.16) | 0.277 |
| TDF, weeks[a] | 60.3 (17.7–115.4) | 73.3 (37.7–109.1) | 0.888 |

*KTD* kidney tubular dysfunction, *β2M* urinary β2-microglobulin, *α1M* urinary α1-microglobulin, *NAG* N-acetyl-β-D-glucosaminidase in urine, $FE_{IP}$ fractional excretion of phosphate, $FE_{UA}$ fractional excretion of uric acid, *eGFR* estimated glomerular filtration rate, *TDF* tenofovir disoproxil fumarate

[a] Median (interquartile range)

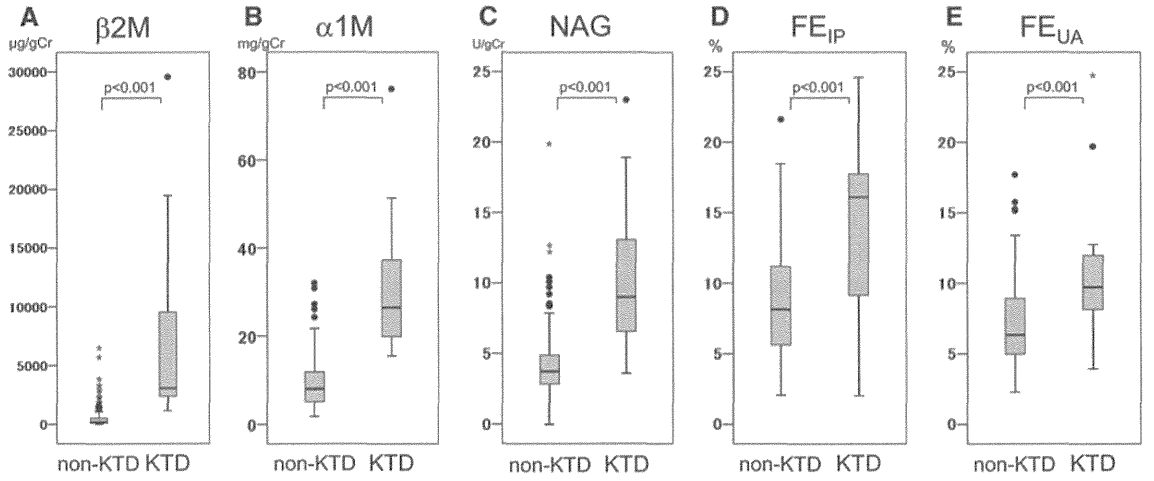


**Fig. 2** Box-and-whisker plots of five tubular markers: urinary β2-microglobulin (*β2M*) (**a**), urinary α1-microglobulin (*α1M*) (**b**), *N*-acetyl-β-D-glucosaminidase in urine (*NAG*) (**c**), fractional excretion of phosphate ($FE_{IP}$) (**d**), and fractional excretion of uric acid ($FE_{UA}$) levels in patients with kidney tubular function (*KTD*) and those with normal tubular function (*non-KTD*) (**e**). In these plots, *lines within the boxes* represent median values; the *upper* and *lower lines of the boxes* represent the 25th and 75th percentiles, respectively; and the *upper and lower bars outside the boxes* represent the maximum and the minimum values or to the most extreme values within 1.5 interquartile ranges of the quartiles, respectively. *Closed circles* and *asterisks* in each graph represent outliers

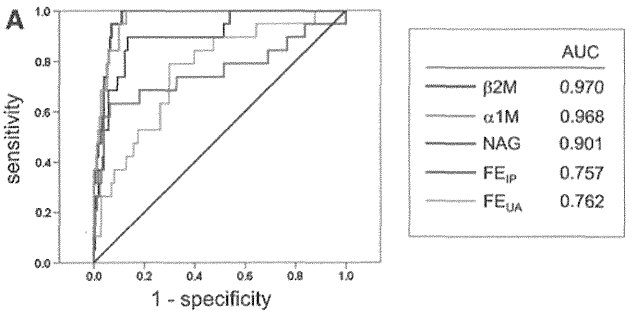


B

| | AUC | 95% CI | Std. Err. | P value | P value† |
|---|---|---|---|---|---|
| β2M (standard) | 0.970 | 0.947-0.992 | 0.011 | | |
| α1M | 0.968 | 0.944-0.992 | 0.012 | 0.886 | 1 |
| NAG | 0.901 | 0.828-0.974 | 0.038 | 0.093 | 0.371 |
| $FE_{IP}$ | 0.757 | 0.607-0.907 | 0.078 | 0.004 | 0.018 |
| $FE_{UA}$ | 0.762 | 0.653-0.872 | 0.057 | <0.001 | <0.001 |

**Fig. 3** The diagnostic accuracy of five tubular markers for tenofovir-induced tubulopathy. **a** Receiver operating characteristic (ROC) curves and areas under the curve (AUC) for five tubular markers. **b** The differences between the largest AUC (β2M) and each of the other AUCs were tested using a nonparametric method. *p* value†, value adjusted with Bonferroni correction

## Discussion

To our knowledge, this is the first study to compare various kidney tubular markers for screening tenofovir-induced KTD in patients with HIV-1 infection. Both urinary β2M and α1M were identified as good screening markers with high diagnostic accuracy among the five tubular markers examined in this study. With a cutoff value of 1,123 μg/g Cr for β2M (sensitivity 100 %, specificity 89 %) and 15.4 mg/g Cr for α1M (sensitivity 100 %, specificity 87 %), these two markers are potentially suited for screening tenofovir-induced KTD. Although these low molecular weight proteins offered good screening ability, both $FE_{IP}$ and $FE_{UA}$, which are traditional tubular function markers often used for the diagnosis of Fanconi syndrome, were not useful for screening KTD. NAG, a lysosomal enzyme of proximal tubular epithelial cells, had good diagnostic accuracy with a cutoff value of 5.96 U/g Cr (sensitivity 90 %, specificity 86 %). However, with cutoff of 3.58 U/g Cr, which yields 100 % sensitivity and maximal specificity, NAG had relatively low specificity of 46 %, and thus has a high false-positive rate.

TDF is one of the most important and widely used agents in the treatment of HIV-1 infection, as well as hepatitis B infection [4]. Fixed-dose tenofovir/emtricitabine is the only preferred NRTI in the American Department of Health and Human Services (DHHS) Guidelines and the revised British HIV Association Guidelines [33, 34]. TDF is also increasingly used in resource-limited settings, following the revised 2010 WHO guidelines that recommend TDF as one of the components of first-line therapies [35]. Although tenofovir nephrotoxicity is considered to be mild and tolerable [9], its long-term consequences are unknown. Thus, it is important to have a useful screening tool for tenofovir-induced nephrotoxicity.

**Table 2** Cutoff values of five kidney tubular markers (calculated with 100 % sensitivity and maximal specificity) and two conventional methods

| | Cutoff with 100 % sensitivity | | | Method 1 | | | Method 2 | | |
|---|---|---|---|---|---|---|---|---|---|
| | Cutoff | Sensitivity (%) | Specificity (%) | Cutoff | Sensitivity (%) | Specificity (%) | Cutoff | Sensitivity (%) | Specificity (%) |
| β2M (μg/g Cr) | 1,123 | 100 | 89 | 1,612 | 95 | 93 | 1,123 | 100 | 89 |
| α1M (mg/g Cr) | 15.4 | 100 | 87 | 16.5 | 95 | 90 | 15.4 | 100 | 87 |
| NAG (U/g Cr) | 3.58 | 100 | 46 | 5.96 | 90 | 86 | 5.96 | 90 | 86 |
| $FE_{IP}$ (%) | 1.02 | 100 | 0 | 12.4 | 68 | 82 | 14.4 | 63 | 94 |
| $FE_{UA}$ (%) | 3.92 | 100 | 12 | 8.1 | 79 | 70 | 8.1 | 79 | 70 |

*β2M* urinary β2-microglobulin, *α1M* urinary α1-microglobulin, *NAG* N-acetyl-β-D-glucosaminidase in urine, $FE_{IP}$ fractional excretion of phosphate, $FE_{UA}$ fractional excretion of uric acid

Previous studies identified old age, low body weight, preexisting renal impairment, concomitant use of nephrotoxic medications, concomitant use of ritonavir-boosted protease inhibitors, advanced HIV infection (low CD4 counts, AIDS), and other comorbidities (diabetes mellitus, hypertension, hepatitis C co-infection) as risk factors for tenofovir-induced reduction in renal function [14, 27–30]. The DHHS Guidelines recommend monitoring eGFR, urinalysis, and electrolytes in patients on TDF [33]. We suggest monitoring either urinary β2M or α1M in addition to the variables recommended by the DHHS guidelines every 6 months in patients under tenofovir use, especially in those with the aforementioned risk factors in resource-rich settings.

One of the strengths of the present study is the exclusion of factors that could otherwise predispose to KTD other than tenofovir, such as active infection, diabetes mellitus, preexisting renal impairment, and HIV-1 viremia, to make prevalence of KTD lower than that in the real-world settings [20]. The cutoff values of tubular markers for screening tenofovir-induced KTD with 100 % sensitivity were calculated in this setting. Thus, in applying these cutoff values in clinical practice with high prevalence rates of KTD, the false-positive rate will be lower than the one reported in the present study, making these cutoff values even more useful.

Another strength of the study is that the enrolled patients were on the same antiretroviral regimen (once-daily ritonavir-boosted darunavir plus fixed-dose tenofovir/emtricitabine). This practice helped proper evaluation of the diagnostic accuracy of the five tubular markers, because plasma concentrations of tenofovir and severity of tenofovir-induced KTD are influenced by concomitant use of antiretrovirals, and the delta change in plasma tenofovir concentration likely differs in the presence of each concomitant drug [36]. Thus, by enrolling patients on the same antiretroviral combination, this study excluded an important confounding factor for tenofovir-induced KTD.

Both β2M and α1M are low molecular weight proteins (<40 kDa) used as markers of kidney tubular function. β2M and the free unbound form of α1M are freely filtered by the glomerulus and reabsorbed almost completely in proximal tubular cells [37]. Serum β2M has been used as a surrogate marker of inflammation, because it is expressed on the surface of most nucleated cells, as part of class I major histocompatibility complex. On the other hand, α1M is mainly produced in the liver, and although its function is not fully understood, it has antioxidant properties and acts as a radical scavenger [38]. Of note, technical difficulty has been reported in the measurement of both markers; for β2M, acidic urine with pH <6.0 causes time- and temperature-dependent degradation of β2M [39]. Urinary α1M is more stable than β2M when stored in acidic urine; however, diurnal variation and gender differences have been reported [40–42].

There are several limitations in this study. First, there is no gold standard definition for KTD. The collection of abnormal tubular markers was used as a reference standard in this study, following their use in previous studies for the diagnosis of KTD [17, 43]. However, the criteria used for the diagnosis of KTD in each previous study included haphazard combination of tubular markers [16, 44]. Accordingly, this study selected five markers (β2M, α1M, NAG, $FE_{IP}$, and $FE_{UA}$) after taking into consideration their availability and cost. Thus, our study did not investigate other tubular markers, such as γ-glutamyl transpeptidase, retinol binding protein, and neutrophil gelatinase-associated lipocalin. Second, although this study evaluated the diagnostic values for five variables (β2M, α1M, NAG, $FE_{IP}$, and $FE_{UA}$), these variables were not fully independent from KTD, the reference standard, because KTD was defined as the collection of abnormal tubular markers [17, 43]. Third, the study subjects were mostly men, and thus the results of this study are not necessarily applicable to women, especially considering that gender variation should be taken into account in evaluation of α1M [40].

In conclusion, the present study identified urinary β2M and α1M as highly useful screening markers for tenofovir-induced KTD, in a setting designed to exclusively evaluate tenofovir-induced KTD. In the assessment of renal function

in patients under tenofovir therapy, regular monitoring of either urinary β2M or α1M, in addition to urinalysis, serum creatinine, and electrolytes, should be helpful in the diagnosis of early-stage tenofovir-induced KTD. Screening for tenofovir-induced KTD is especially important in patients with several risk factors for KTD, because undetected long-term tubular dysfunction might lead to premature osteopenia caused by phosphate wasting, and accelerated progression of renal dysfunction, both of which could result in a serious outcome.

**Acknowledgments** The authors thank all the patients who participated in the study, and Fumihiko Hinoshita, Hirohisa Yazaki, Haruhito Honda, Ei Kinai, Koji Watanabe, Takahiro Aoki, Daisuke Mizushima, Yohei Hamada, Michiyo Ishisaka, Mikiko Ogata, Minami Takahashi, and Akiko Nakano, and all other clinical staff at the AIDS Clinical Center for their help in completion of this study. This work was supported by a Grant-in Aid for AIDS research from the Japanese Ministry of Health, Labour, and Welfare (H23-AIDS-001), and the Global Center of Excellence Program (Global Education and Research Center Aiming at the Control of AIDS) from the Japanese Ministry of Education, Science, Sports and Culture. The funders had no role in study design, data collection and analysis, decision to publish, or preparation of the manuscript.

**Conflict of interest** Shinichi Oka has received a research grant from MSD K.K., Abbott Japan Co., Janssen Pharmaceutical K.K., Pfizer Co., and Roche Diagnostics K.K. The other authors declare no conflict of interest.

## References

1. Sax PE, Tierney C, Collier AC, Daar ES, Mollan K, Budhathoki C, et al. Abacavir/lamivudine versus tenofovir DF/emtricitabine as part of combination regimens for initial treatment of HIV: final results. J Infect Dis. 2011;204:1191–201.
2. Post FA, Moyle GJ, Stellbrink HJ, Domingo P, Podzamczer D, Fisher M, et al. Randomized comparison of renal effects, efficacy, and safety with once-daily abacavir/lamivudine versus tenofovir/emtricitabine, administered with efavirenz, in antiretroviral-naive, HIV-1-infected adults: 48-week results from the ASSERT study. J Acquir Immune Defic Syndr. 2010;55:49–57.
3. Arribas JR, Pozniak AL, Gallant JE, Dejesus E, Gazzard B, Campo RE, et al. Tenofovir disoproxil fumarate, emtricitabine, and efavirenz compared with zidovudine/lamivudine and efavirenz in treatment-naive patients: 144-week analysis. J Acquir Immune Defic Syndr. 2008;47:74–8.
4. Woo G, Tomlinson G, Nishikawa Y, Kowgier M, Sherman M, Wong DK, et al. Tenofovir and entecavir are the most effective antiviral agents for chronic hepatitis B: a systematic review and Bayesian meta-analyses. Gastroenterology. 2010;139:1218–29.
5. Verhelst D, Monge M, Meynard JL, Fouqueray B, Mougenot B, Girard PM, et al. Fanconi syndrome and renal failure induced by tenofovir: a first case report. Am J Kidney Dis. 2002;40:1331–3.
6. Schaaf B, Aries SP, Kramme E, Steinhoff J, Dalhoff K. Acute renal failure associated with tenofovir treatment in a patient with acquired immunodeficiency syndrome. Clin Infect Dis. 2003;37:e41–3.
7. Peyriere H, Reynes J, Rouanet I, Daniel N, de Boever CM, Mauboussin JM, et al. Renal tubular dysfunction associated with tenofovir therapy: report of 7 cases. J Acquir Immune Defic Syndr. 2004;35:269–73.
8. Nishijima T, Gatanaga H, Komatsu H, Tsukada K, Shimbo T, Aoki T, et al. Renal function declines more in tenofovir- than abacavir-based antiretroviral therapy in low-body weight treatment-naive patients with HIV infection. PLoS ONE. 2012;7:e29977.
9. Cooper RD, Wiebe N, Smith N, Keiser P, Naicker S, Tonelli M. Systematic review and meta-analysis: renal safety of tenofovir disoproxil fumarate in HIV-infected patients. Clin Infect Dis. 2010;51:496–505.
10. Fux CA, Rauch A, Simcock M, Bucher HC, Hirschel B, Opravil M, et al. Tenofovir use is associated with an increase in serum alkaline phosphatase in the Swiss HIV cohort study. Antivir Ther. 2008;13:1077–82.
11. McComsey GA, Kitch D, Daar ES, Tierney C, Jahed NC, Tebas P, et al. Bone mineral density and fractures in antiretroviral-naive persons randomized to receive abacavir-lamivudine or tenofovir disoproxil fumarate-emtricitabine along with efavirenz or atazanavir-ritonavir: AIDS Clinical Trials Group A5224s, a substudy of ACTG A5202. J Infect Dis. 2011;203:1791–801.
12. Gallant JE, Winston JA, DeJesus E, Pozniak AL, Chen SS, Cheng AK, et al. The 3-year renal safety of a tenofovir disoproxil fumarate vs. a thymidine analogue-containing regimen in antiretroviral-naive patients. AIDS. 2008;22:2155–63.
13. Izzedine H, Hulot JS, Vittecoq D, Gallant JE, Staszewski S, Launay-Vacher V, et al. Long-term renal safety of tenofovir disoproxil fumarate in antiretroviral-naive HIV-1-infected patients. Data from a double-blind randomized active-controlled multicentre study. Nephrol Dial Transplant. 2005;20:743–6.
14. Gatanaga H, Tachikawa N, Kikuchi Y, Teruya K, Genka I, Honda M, et al. Urinary beta2-microglobulin as a possible sensitive marker for renal injury caused by tenofovir disoproxil fumarate. AIDS Res Hum Retroviruses. 2006;22:744–8.
15. Papaleo A, Warszawski J, Salomon R, Jullien V, Veber F, Dechaux M, et al. Increased beta-2 microglobulinuria in human immunodeficiency virus-1-infected children and adolescents treated with tenofovir. Pediatr Infect Dis J. 2007;26:949–51.
16. Han WK, Wagener G, Zhu Y, Wang S, Lee HT. Urinary biomarkers in the early detection of acute kidney injury after cardiac surgery. Clin J Am Soc Nephrol. 2009;4:873–82.
17. Izzedine H, Hulot JS, Villard E, Goyenvalle C, Dominguez S, Ghosn J, et al. Association between ABCC2 gene haplotypes and tenofovir-induced proximal tubulopathy. J Infect Dis. 2006;194:1481–91.
18. Rodriguez-Novoa S, Labarga P, Soriano V, Egan D, Albalater M, Morello J, et al. Predictors of kidney tubular dysfunction in HIV-infected patients treated with tenofovir: a pharmacogenetic study. Clin Infect Dis. 2009;48:e108–16.
19. Han WK, Waikar SS, Johnson A, Betensky RA, Dent CL, Devarajan P, et al. Urinary biomarkers in the early diagnosis of acute kidney injury. Kidney Int. 2008;73:863–9.
20. Ando M, Yanagisawa N, Ajisawa A, Tsuchiya K, Nitta K. Kidney tubular damage in the absence of glomerular defects in HIV-infected patients on highly active antiretroviral therapy. Nephrol Dial Transplant. 2011;26:3224–9.
21. Bossuyt PM, Reitsma JB, Bruns DE, Gatsonis CA, Glasziou PP, Irwig LM, et al. Towards complete and accurate reporting of studies of diagnostic accuracy: the STARD Initiative. Ann Intern Med. 2003;138:40–4.
22. Nishijima T, Komatsu H, Higasa K, Takano M, Tsuchiya K, Hayashida T, et al. Single nucleotide polymorphisms in ABCC2 associate with tenofovir-induced kidney tubular dysfunction in Japanese patients with HIV-1 infection: a pharmacogenetic study. Clin Infect Dis. 2012;55(11):1558–67.
23. Cockcroft DW, Gault MH. Prediction of creatinine clearance from serum creatinine. Nephron. 1976;16:31–41.
24. Carrieri M, Trevisan A, Bartolucci GB. Adjustment to concentration-dilution of spot urine samples: correlation between

specific gravity and creatinine. Int Arch Occup Environ Health. 2001;74:63–7.
25. Salem MA, el-Habashy SA, Saeid OM, el-Tawil MM, Tawfik PH. Urinary excretion of *N*-acetyl-beta-D-glucosaminidase and retinol binding protein as alternative indicators of nephropathy in patients with type 1 diabetes mellitus. Pediatr Diabetes. 2002;3: 37–41.
26. Ezinga M, Wetzels J, van der Ven A, Burger D. Kidney tubular dysfunction is related to tenofovir plasma concentration (abstract 603). In: Program and abstracts of the 19th Conference on Retroviruses and Opportunistic Infections, 5–8 March, 2012, Seattle, WA
27. Gupta SK, Eustace JA, Winston JA, Boydstun II, Ahuja TS, Rodriguez RA, et al. Guidelines for the management of chronic kidney disease in HIV-infected patients: recommendations of the HIV Medicine Association of the Infectious Diseases Society of America. Clin Infect Dis. 2005;40:1559–85.
28. Goicoechea M, Liu S, Best B, Sun S, Jain S, Kemper C, et al. Greater tenofovir-associated renal function decline with protease inhibitor-based versus nonnucleoside reverse-transcriptase inhibitor-based therapy. J Infect Dis. 2008;197:102–8.
29. Nelson MR, Katlama C, Montaner JS, Cooper DA, Gazzard B, Clotet B, et al. The safety of tenofovir disoproxil fumarate for the treatment of HIV infection in adults: the first 4 years. AIDS. 2007;21:1273–81.
30. Fernandez-Fernandez B, Montoya-Ferrer A, Sanz AB, Sanchez-Nino MD, Izquierdo MC, Poveda J, et al. Tenofovir nephrotoxicity: 2011 update. AIDS Res Treat. 2011;2011:354908.
31. DeLong ER, DeLong DM, Clarke-Pearson DL. Comparing the areas under two or more correlated receiver operating characteristic curves: a nonparametric approach. Biometrics. 1988;44: 837–45.
32. Perkins NJ, Schisterman EF. The inconsistency of "optimal" cutpoints obtained using two criteria based on the receiver operating characteristic curve. Am J Epidemiol. 2006;163:670–5.
33. Panel on Antiretroviral Guidelines for Adults and Adolescents. Guidelines for the use of antiretroviral agents in HIV-1-infected adults and adolescents. Department of Health and Human Services. 1–239. Available at http://www.aidsinfo.nih.gov/ContentFiles/AdultandAdolescentGL.pdf. Accessed 7 June 2012.
34. The BHIVA Treatment Guidelines Writing Group. BHIVA guidelines for the treatment of HIV-1 positive adults with antiretroviral therapy 2012. British HIV Association. 1–139. Available at http://www.bhiva.org/documents/Guidelines/Treatment/2012/120430TreatmentGuidelines.pdf. Accessed 15 June 2012.
35. Antiretroviral therapy for HIV infection in adults and adolescents Recommendations for a public health approach 2010 revision. World Health Organization. 1–156. Available at http://whqlibdoc.who.int/publications/2010/9789241599764_eng.pdf. Accessed 7 June 2012.
36. Kiser JJ, Carten ML, Aquilante CL, Anderson PL, Wolfe P, King TM, et al. The effect of lopinavir/ritonavir on the renal clearance of tenofovir in HIV-infected patients. Clin Pharmacol Ther. 2008;83:265–72.
37. Lisowska-Myjak B. Serum and urinary biomarkers of acute kidney injury. Blood Purif. 2010;29:357–65.
38. Olsson MG, Centlow M, Rutardottir S, Stenfors I, Larsson J, Hosseini-Maaf B, et al. Increased levels of cell-free hemoglobin, oxidation markers, and the antioxidative heme scavenger alpha(1)-microglobulin in preeclampsia. Free Radic Biol Med. 2010;48:284–91.
39. Hong CY, Chia KS. Markers of diabetic nephropathy. J Diabetes Complications. 1998;12:43–60.
40. Andersson L, Haraldsson B, Johansson C, Barregard L. Methodological issues on the use of urinary alpha-1-microglobuline in epidemiological studies. Nephrol Dial Transplant. 2008;23: 1252–6.
41. Tencer J, Thysell H, Andersson K, Grubb A. Long-term stability of albumin, protein HC, immunoglobulin G, kappa- and lambda-chain-immunoreactivity, orosomucoid and alpha 1-antitrypsin in urine stored at −20 degrees C. Scand J Urol Nephrol. 1997;31: 67–71.
42. Itoh Y, Kawai T. Human alpha 1-microglobulin: its measurement and clinical significance. J Clin Lab Anal. 1990;4:376–84.
43. Rodriguez-Novoa S, Labarga P, Soriano V. Pharmacogenetics of tenofovir treatment. Pharmacogenomics. 2009;10:1675–85.
44. Rodriguez-Novoa S, Alvarez E, Labarga P, Soriano V. Renal toxicity associated with tenofovir use. Expert Opin Drug Saf. 2010;9:545–59.

INTERNAL MEDICINE

□ CASE REPORT □

# Idiopathic Oropharyngeal and Esophageal Ulcers Related to HIV Infection Successfully Treated with Antiretroviral Therapy Alone

Yohei Hamada[1], Naoyoshi Nagata[2], Haruhito Honda[1], Katsuji Teruya[1], Hiroyuki Gatanaga[1], Yoshimi Kikuchi[1] and Shinichi Oka[1]

## Abstract

We herein report the case of an HIV-positive man who was diagnosed with idiopathic esophageal and oropharyngeal ulceration. The esophageal and oropharyngeal ulcers were considered to be idiopathic and related to HIV infection after excluding the possibility of infection with known pathogens. Both the esophageal and oropharyngeal ulcers showed significant improvements following antiretroviral therapy alone. Idiopathic esophageal ulcers are a well-known complication of late-stage HIV infection. However, involvement of both the esophagus and pharynx is rare. Furthermore, antiretroviral therapy without concomitant steroids is effective against idiopathic esophageal and oropharyngeal ulcers related to HIV infection.

**Key words:** HIV infection, idiopathic esophageal ulcer, pharyngeal ulcer, antiretroviral therapy, gastrointestinal diseases

**(Intern Med 52: 393-395, 2013)**
**(DOI: 10.2169/internalmedicine.52.8709)**

## Introduction

Esophageal ulceration is a common complication in patients with human immunodeficiency virus-1 (HIV) infection, especially in the late stage. Although esophageal ulcerations can be caused by various infectious agents, such as *Candida* species, cytomegalovirus (CMV) and herpes simplex virus (HSV), a large proportion of patients are diagnosed with idiopathic esophageal ulcerations (1, 2) with no detectable etiology. Oropharyngeal ulcers are also an important comorbidity that can become progressive in HIV-infected patients (3, 4). The common infectious agents of esophageal ulcerations are known to also cause oropharyngeal ulcerations, although some cases are considered idiopathic with no identifiable etiology (5, 6). However, simultaneous involvement of the esophagus and oropharynx is uncommon outside of HSV esophagitis (5). We herein report a case of unusual discrete ulcers of the oropharynx and esophagus in a patient with HIV infection that showed a rapid improvement following treatment with antiretroviral therapy alone.

## Case Report

A previously healthy 60-year-old Japanese homosexual man presented with severe odynophagia. He was diagnosed with oral candidiasis and HIV infection and therefore had been referred to our hospital (day-1). Laboratory tests showed a low CD4+ cell count (49/μL), a high HIV-RNA titer ($1.0\times10^6$ copies/mL) and a low serum albumin level (Alb 2.9 g/dL). Whole-blood polymerase chain reaction (PCR) was negative for both CMV and HSV. The patient was treated with fluconazole for seven days for suspected esophageal candidiasis. Despite this treatment, the odynophagia did not improve. Since oral ulcers were noticed, treatment with oral valaciclovir at a dose of 1,000 mg/day was initiated based on a presumptive diagnosis of HSV infection. However, the odynophagia persisted, and the oral ulcers did not show any improvement despite a 3-week

[1]AIDS Clinical Center, National Center for Global Health and Medicine, Japan and [2]Department of Gastroenterology, National Center for Global Health and Medicine, Japan
Received for publication July 30, 2012; Accepted for publication October 30, 2012
Correspondence to Dr. Naoyoshi Nagata, nnagata_ncgm@yahoo.co.jp

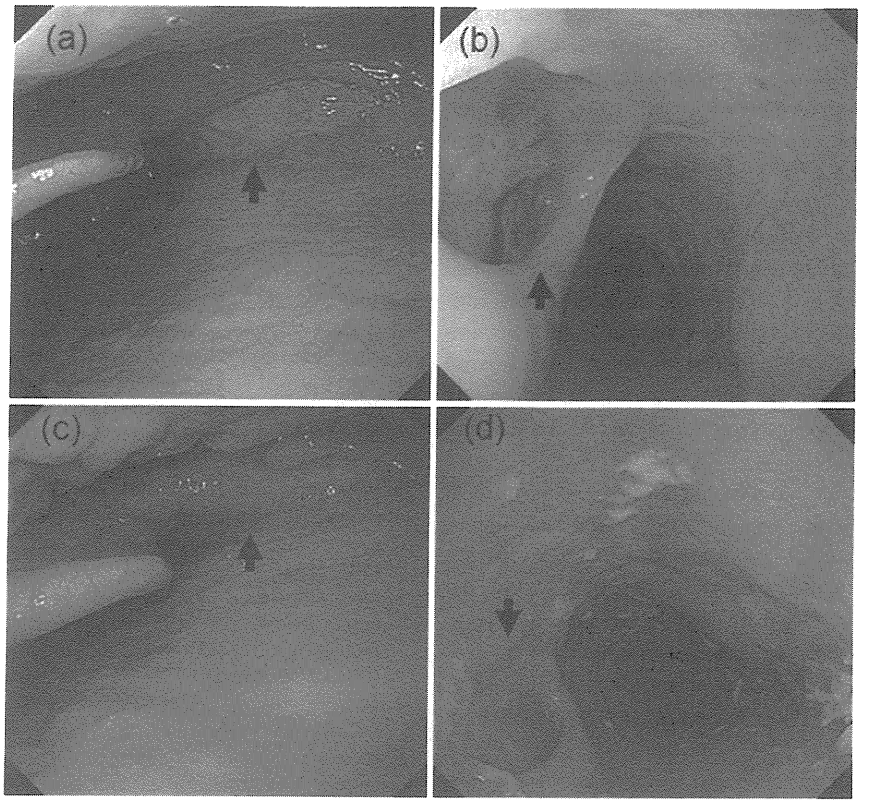


**Figure. Endoscopic findings of the pharynx and esophagus. The pharyngeal (a) and esophageal (b) ulcers before the administration of antiretroviral therapy. The endoscopic appearance of the pharynx (c) and esophagus (d) on day 22 of antiretroviral therapy. Black arrows: ulcers.**

course of anti-HSV therapy; thus, upper gastrointestinal endoscopy was performed. Endoscopy showed large, discrete and well-circumscribed esophageal and pharyngeal ulcers (Figure a, b). Because a diagnosis of CMV esophagitis was suspected based on the endoscopic appearance of the ulcers, treatment with intravenous gancicrovir at a dose of 5 mg/kg every 12 hours was initiated and the valaciclovir was discontinued. However, a histopathological examination of the biopsy specimen obtained from the base and edge of an ulcer before the initiation of gancicrovir therapy revealed lymphocytic infiltration without intranuclear or intracytoplasmic inclusion bodies. Immunohistochemical staining for CMV and HSV was negative. PCR assays of both pharyngeal and esophageal biopsies were negative for CMV-DNA and HSV-DNA (≤40 copies/μg DNA). Furthermore, repeat endoscopy performed after two weeks of gancicrovir therapy showed exacerbation of the ulcers. Based on these findings, we administered antiretroviral therapy consisting of ritonavir-boosted darunavir with abacavir/lamivudine. The gancicrovir therapy was discontinued after the completion of a 3-week course of treatment. The odynophagia gradually improved and ultimately disappeared two weeks later, while the CD4 count increased to 91/μL and the HIV-RNA titer decreased to $4\times10^4$ copies/mL. Endoscopy performed on day 22 of antiretroviral therapy demonstrated significant reductions in the size and depth of the pharyngeal and esophageal ulcers (Figure c, d). Additionally, resolution of the oral ulcers was noticed.

## Discussion

To our knowledge, this is the first report of idiopathic esophageal and oropharyngeal ulcers successfully treated with antiretroviral therapy alone in a patient with late-stage HIV infection. Steroids are commonly used as the standard treatment for idiopathic esophageal ulcers (2, 7). However, steroids can lead to serious opportunistic infections due to their immunosuppressive effects. The efficacy of steroids is mostly based on reports from the pre-highly active antiretroviral therapy era, and the efficacy of antiretroviral therapy has not been examined. As described above, steroid therapy may not be necessary when a potent combination of antiretroviral therapy is administered. The etiology of idiopathic esophageal ulcers is still not fully understood. Although such ulcers are considered to be associated with HIV infection, they have been referred to as idiopathic when no identifiable etiologic agent other than HIV infection is present (8, 9). The potential pathogenesis of these ulcers includes apoptosis of the esophageal mucosa induced by HIV infection (10). Based on this probable pathogenesis, it is therefore considered to be rational to administer antiretroviral therapy to treat idiopathic esophageal ulcers.

The diagnosis of idiopathic oropharyngeal and esophageal ulcers is established by excluding other infectious agents known to cause esophageal ulceration, including CMV, HSV and *Candida* sp, by performing histopathological and immunological examinations of biopsy specimens (1, 2, 5, 6). In our case, the histopathological findings showed no evidence of any infectious pathogens, and CMV and HSV infection were also excluded by PCR assays, which have a high sensitivity (11, 12). Furthermore, the oropharyngeal and esophageal ulcers were refractory to anti-CMV and anti-HSV therapy. In addition, the ulcers showed significant improvement following the administration of antiretroviral therapy alone. Therefore, the final diagnosis was idiopathic oropharyngeal and esophageal ulcers related to HIV infection.

Involvement of both the oropharynx and esophagus in HSV-related ulcers is not uncommon (5). However, in our patient, the esophageal and oropharyngeal ulcers were considered idiopathic, which is extremely rare. In this case, the ulcers in both regions were examined endoscopically. Therefore, performing careful endoscopic examinations of not only the esophagus, but also the pharynx, is considered to be important for establishing the cause of odynophagia in HIV-infected patients.

In conclusion, a pharyngeal and esophageal biopsy obtained using upper gastrointestinal endoscopy was useful for establishing the diagnosis in this case. Furthermore, antiretroviral therapy alone resulted in a significant improvement of the idiopathic ulcers in our HIV-infected patient. The initiation of antiretroviral therapy without steroids is therefore a reasonable option for treating idiopathic oropharyngeal and esophageal ulcers in HIV-infected patients.

**The authors state that they have no Conflict of Interest (COI).**

**Acknowledgement**

The authors thank Toru Igari for valuable help in performing the histopathological examination and the entire clinical staff at the AIDS Clinical Center. We also thank the staff of the endoscopy unit.

## References

1. Bonacini M, Young T, Laine L. The causes of esophageal symptoms in human immunodeficiency virus infection. A prospective study of 110 patients. Arch Intern Med **151**: 1567-1572, 1991.
2. Wilcox CM, Schwartz DA, Clark WS. Esophageal ulceration in human immunodeficiency virus infection. Causes, response to therapy, and long-term outcome. Ann Intern Med **123**: 143-149, 1995.
3. Gorin I, Vilette B, Gehanno P, Escande JP. Thalidomide in hyperalgic pharyngeal ulceration of AIDS. Lancet **335**: 1343, 1990.
4. MacPhail LA, Greenspan D, Feigal DW, Lennette ET, Greenspan JS. Recurrent aphthous ulcers in association with HIV infection. Description of ulcer types and analysis of T-lymphocyte subsets. Oral Surg Oral Med Oral Pathol **71**: 678-683, 1991.
5. Wilcox CM, Straub RF, Clark WS. Prospective evaluation of oropharyngeal findings in human immunodeficiency virus-infected patients with esophageal ulceration. Am J Gastroenterol **90**: 1938-1941, 1995.
6. Liang GS, Daikos GL, Serfling U, et al. An evaluation of oral ulcers in patients with AIDS and AIDS-related complex. J Am Acad Dermatol **29**: 563-568, 1993.
7. Wilcox CM, Schwartz DA. Comparison of two corticosteroid regimens for the treatment of HIV-associated idiopathic esophageal ulcer. Am J Gastroenterol **89**: 2163-2167, 1994.
8. Bhaijee F, Subramony C, Tang SJ, Pepper DJ. Human immunodeficiency virus-associated gastrointestinal disease: common endoscopic biopsy diagnoses. Patholog Res Int **2011**: 247923, 2011.
9. Nishijima T, Tsukada K, Nagata N, et al. Antiretroviral therapy alone resulted in successful resolution of large idiopathic esophageal ulcers in a patient with acute retroviral syndrome. AIDS **25**: 1677-1679, 2011.
10. Houghton JM, Korah RM, Kim KH, Small MB. A role for apoptosis in the pathogenesis of AIDS-related idiopathic esophageal ulcers. J Infect Dis **175**: 1216-1219, 1997.
11. Jazeron JF, Barbe C, Frobert E, et al. Virological diagnosis of herpes simplex virus 1 esophagitis by quantitative real-time PCR assay. J Clin Microbiol **50**: 948-952, 2012.
12. Reddy N, Wilcox CM. Diagnosis & management of cytomegalovirus infections in the GI tract. Expert Rev Gastroenterol Hepatol **1**: 287-294, 2007.

JVI Journals.ASM.org

# Distinct HIV-1 Escape Patterns Selected by Cytotoxic T Cells with Identical Epitope Specificity

Yuichi Yagita,[a] Nozomi Kuse,[a] Kimiko Kuroki,[b] Hiroyuki Gatanaga,[a,c] Jonathan M. Carlson,[d] Takayuki Chikata,[a] Zabrina L. Brumme,[e,f] Hayato Murakoshi,[a] Tomohiro Akahoshi,[a] Nico Pfeifer,[d] Simon Mallal,[g] Mina John,[g] Toyoyuki Ose,[b] Haruki Matsubara,[b] Ryo Kanda,[b] Yuko Fukunaga,[b] Kazutaka Honda,[a] Yuka Kawashima,[a] Yasuo Ariumi,[a] Shinichi Oka,[a,c] Katsumi Maenaka,[b] Masafumi Takiguchi[a]

Center for AIDS Research, Kumamoto University, Chuo-ku, Kumamoto, Japan[a]; Laboratory of Biomolecular Science, Faculty of Pharmaceutical Sciences, Hokkaido University, Kita-ku, Sapporo, Japan[b]; AIDS Clinical Center, National Center for Global Health and Medicine, Shinjuku-ku, Tokyo, Japan[c]; eScience Group, Microsoft Research, Los Angeles, California[d]; Faculty of Health Sciences, Simon Fraser University, Burnaby BC, Canada[e]; British Columbia Centre for Excellence in HIV/AIDS, Vancouver, BC, Canada[f]; Institute for Immunology & Infectious Diseases, Murdoch University, Murdoch, Western Australia, Australia[g]

**Pol283-8-specific, HLA-B*51:01-restricted, cytotoxic T cells (CTLs) play a critical role in the long-term control of HIV-1 infection. However, these CTLs select for the reverse transcriptase (RT) I135X escape mutation, which may be accumulating in circulating HIV-1 sequences. We investigated the selection of the I135X mutation by CTLs specific for the same epitope but restricted by HLA-B*52:01. We found that Pol283-8-specific, HLA-B*52:01-restricted CTLs were elicited predominantly in chronically HIV-1-infected individuals. These CTLs had a strong ability to suppress the replication of wild-type HIV-1, though this ability was weaker than that of HLA-B*51:01-restricted CTLs. The crystal structure of the HLA-B*52:01-Pol283-8 peptide complex provided clear evidence that HLA-B*52:01 presents the peptide similarly to HLA-B*51:01, ensuring the cross-presentation of this epitope by both alleles. Population level analyses revealed a strong association of HLA-B*51:01 with the I135T mutant and a relatively weaker association of HLA-B*52:01 with several I135X mutants in both Japanese and predominantly Caucasian cohorts. An *in vitro* viral suppression assay revealed that the HLA-B*52:01-restricted CTLs failed to suppress the replication of the I135X mutant viruses, indicating the selection of these mutants by the CTLs. These results suggest that the different pattern of I135X mutant selection may have resulted from the difference between these two CTLs in the ability to suppress HIV-1 replication.**

HIV-1-specific cytotoxic T cells (CTLs) play an important role in the control of HIV-1 replication (1–8); however, they also select immune escape mutations (9, 10). Population level adaptation of HIV to human leukocyte antigen (HLA) has been demonstrated (11–15), suggesting that HIV-1 can successfully adapt to immune responses previously effective against it.

It is well known that particular mutations can be selected by CTLs specific for a single HIV-1 epitope. On the other hand, studies on HLA-associated HIV-1 polymorphisms have revealed examples of particular mutations associated with multiple HLA class I alleles (16–21), suggesting that the same mutation can be selected by CTLs carrying different specificities in some cases. However, the selection of the same mutation by CTLs specific for different HIV-1 epitopes has rarely been reported. The change from Ala to Pro at residue 146 of Gag (A146P) is a well-analyzed case. A146P is an escape selected by not only HLA-B*57-restricted, ISW9-specific CTLs (22) but also by HLA-B*15:10-restricted and HLA-B*48:01-restricted CTLs (15, 23, 24), although the latter CTLs selected it by different mechanisms. The replacement of Thr with Asn at residue 242 (T242N) of Gag is another case. This mutant is selected by HLA-B*58:01-restricted and HLA-B*57-restricted CTLs specific for the TW10 epitope in HIV-1 clade B- and C-infected individuals (25–27).

The presence of Pol283-8(TAFTIPSI: TI8)-specific, HLA-B*51:01-restricted CTLs is associated with low viral loads in HIV-1-infected Japanese hemophiliacs, supporting an important role in the long-term control of HIV-1 infection (28). We previously showed that the frequency of a mutation at position 135 (I135X) of reverse transcriptase (RT) is strongly correlated with the prevalence of HLA-B*51 among nine cohorts worldwide and that this mutation is selected by Pol283-8(TAFTIPSI: TI8)-specific, HLA-B*51:01-restricted CTLs (15). Of these cohorts, a Japanese one showed the highest frequency of the I135X mutation in HLA-B*51:01 negatives (66% in a Japanese cohort and 11 to 29% in other cohorts). This finding may be explained by the fact that the Japanese cohort has the highest prevalence of HLA-B*51:01 among these cohorts. Another possibility is that this mutation is selected by HIV-1-specific CTLs restricted by other HLA alleles, which are highly frequent among Japanese individuals but infrequent in or absent from other populations. To clarify the latter possibility, we first analyzed the association of the I135X mutation with other HLA class I alleles in a Japanese cohort and found this mutation also to be associated with HLA-B*52:01. We next sought to identify an HLA-B*52:01-restricted CTL epitope including RT135 and found that both HLA-B*51:01 and -B*52:01 can present the same epitope, Pol283-8. Using population level analyses of Japanese and Caucasian cohorts, we identified HLA-B*51:01- and HLA-B*52:01-specific polymorphisms at RT codon 135 (position 8 of this epitope) and characterized differential pathways of escape between these two alleles. In addition, we assessed the *in vitro* ability of HLA-B*52:01- and HLA-B*51:01-restricted CTLs to se-

Received 20 September 2012 Accepted 26 November 2012
Published ahead of print 12 December 2012
Address correspondence to Masafumi Takiguchi, masafumi@kumamoto-u.ac.jp.
Y.Y., N.K., and K.K. contributed equally to this study.
Supplemental material for this article may be found at http://dx.doi.org/10.1128/JVI.02572-12.

doi:10.1128/JVI.02572-12

lect I135X mutants and elucidated the crystal structure of the HLA-B*52:01-Pol283-8 peptide complex.

## MATERIALS AND METHODS

**Patients.** Two hundred fifty-seven chronically HIV-1-infected, antiretroviral-naïve Japanese individuals were recruited for the present study, which was approved by the ethics committees of Kumamoto University and the National Center for Global Health and Medicine, Japan. Written informed consent was obtained from all subjects according to the Declaration of Helsinki.

In addition, HLA-associated immune selection pressure at RT codon 135 was investigated in the International HIV Adaptation Collaborative (IHAC) cohort, comprising >1,200 chronically HIV-infected, antiretroviral-naïve individuals from Canada, the United States, and Western Australia (19). The majority of the IHAC participants were Caucasian, and the HIV subtype distribution was >95% subtype B.

**HIV-1 clones.** An infectious proviral clone of HIV-1, pNL-432, and its mutant form pNL-M20A (containing a substitution of Ala for Met at residue 20 of Nef) were previously reported (29). Pol283-8 mutant viruses (Pol283-8L, -8T, -8V, and 8R) were previously generated on the basis of pNL-432 (15, 28).

**Generation of CTL clones.** Pol283-8-specific, HLA-B*52:01-restricted CTL clones were generated from HIV-1-specific, bulk-cultured T cells by limiting dilution in U-bottom 96-well microtiter plates (Nunc, Roskilde, Denmark). Each well contained 200 μl of the cloning mixture (about $1 \times 10^6$ irradiated allogeneic peripheral blood mononuclear cells (PBMCs) from healthy donors and $1 \times 10^5$ irradiated C1R-B*52:01 cells prepulsed with the corresponding peptide at 1 μM in RPMI 1640 supplemented with 10% human plasma and 200 U/ml human recombinant interleukin-2).

**Intracellular cytokine staining (ICS) assay.** PBMCs from HIV-1-seropositive HLA-B*52:01$^+$ HLA-B*51:01$^-$ individuals were cultured with each peptide (1 μM). Two weeks later, the cultured cells were stimulated with C1R-B*52:01 cells or those prepulsed with Pol283-8 peptide (1 μM) for 60 min, and then they were washed twice with RPMI 1640 containing 10% fetal calf serum (RPMI 1640-10% FCS). Subsequently, brefeldin A (10 μg/ml) was added. After these cells had been incubated for 6 h, they were stained with an anti-CD8 monoclonal antibody (MAb; Dako Corporation, Flostrup, Denmark), fixed with 4% paraformaldehyde, and then permeabilized with permeabilization buffer. Thereafter, the cells were stained with an anti-gamma interferon (IFN-γ) MAb (BD Bioscience). The percentage of CD8$^+$ cells positive for intracellular IFN-γ was analyzed by using a FACS-Cant II (BD Biosciences, San Jose, CA). All flow cytometric data were analyzed with FlowJo software (Tree Star, Inc., Ashland, OR).

**Identification of 11-mer peptide recognized by HLA-B*52:01-restricted CD8$^+$ T cells.** We identified an 11-mer peptide recognized by HLA-B*52:01-restricted CD8$^+$ T cells as follows. We stimulated PBMCs from a chronically HIV-1-infected HLA-B*52:01$^+$ donor (KI-069) with a peptide cocktail including overlapping 17-mer peptides covering RT135 and cultured the cells for 14 days. The cells in bulk culture were assessed by performing an ICS assay for C1R-HLA-B*52:01 cells prepulsed with each of these 17-mer peptides. The bulk-cultured cells recognized the target cells prepulsed with two of the 17-mer peptides assessed, Pol17-47 (KDFRKYTAFTIPSINNE) and Pol17-48 (TAFTIPSINNETPGIRT). Further analysis with 11-mer overlapping peptides covering the Pol17-48 sequence showed that these bulk-cultured cells recognized the target cells prepulsed with Pol11-142 (TAFTIPSINNE) but not those prepulsed with Pol11-143 (FTIPSINNETP).

**Assay of cytotoxicity of CTL clones to target cells prepulsed with the epitope peptide or infected with a vaccinia virus–HIV-1 recombinant.** The cytotoxicity of Pol283-8-specific, HLA-B*52:01-restricted CTL clones to C1R cells expressing HLA-B*52:01 (C1R-B*52:01), which were previously generated (30), and prepulsed with peptide or infected with a vaccinia virus-HIV-1Gag/Pol recombinant was determined by the standard $^{51}$Cr release assay described previously (31). In brief, the infected cells were incubated with 150 μCi $Na_2{}^{51}CrO_4$ in saline for 60 min and then washed three times with RPMI 1640 medium containing 10% newborn calf serum. Labeled target cells ($2 \times 10^3$/well) were added to each well of a U-bottom 96-well microtiter plate (Nunc, Roskilde, Denmark) with the effector cells at an effector-to-target (E/T) cell ratio of 2:1. The cells were then incubated for 6 h at 37°C. The supernatants were collected and analyzed with a gamma counter. Spontaneous $^{51}$Cr release was determined by measuring the number of counts per minute (cpm) in supernatants from wells containing only target cells (cpm spn). Maximum $^{51}$Cr release was determined by measuring the cpm in supernatants from wells containing target cells in the presence of 2.5% Triton X-100 (cpm max). Specific lysis was defined as (cpm exp − cpm spn)/(cpm max − cpm spn) × 100, where cpm exp is the number of cpm in the supernatant in the wells containing both target and effector cells.

**Enzyme-linked immunospot (ELISPOT) assay.** Cryopreserved PBMCs of chronically HIV-1-infected HLA-B*52:01$^+$ individuals were plated in 96-well polyvinylidene plates (Millipore, Bedford, MA) that had been precoated with 5 μg/ml anti-IFN-γ MAb 1-DIK (Mabtech, Stockholm, Sweden). The appropriate amount of each peptide (100 or 10 nM) was added in a volume of 50 μl, and then PBMCs were added at $1 \times 10^5$ cells/well in a volume of 100 μl. The plates were incubated for 40 h at 37°C in 5% $CO_2$ and then washed with phosphate-buffered saline (PBS) before the addition of biotinylated anti-IFN-γ MAb (Mabtech) at 1 μg/ml. After the plates had been incubated at room temperature for 100 min and then washed with PBS, they were incubated with streptavidin-conjugated alkaline phosphatase (Mabtech) for 40 min at room temperature. Individual cytokine-producing cells were detected as dark spots after a 20-min reaction with 5-bromo-4-chloro-3-indolylphosphate and nitroblue tetrazolium by using an alkaline phosphatase-conjugate substrate (Bio-Rad, Richmond, CA). The spots were counted by an Eliphoto-Counter (Minerva Teck, Tokyo, Japan). PBMCs without peptide stimulation were used as a negative control. Positive responses were defined as those greater than the mean of the negative-control wells plus 2 standard deviations (SD) (the number of spots in wells without peptides).

**HIV-1 replication suppression assay.** The ability of HIV-1-specific CTLs to suppress HIV-1 replication was examined as previously described (32). CD4$^+$ T cells isolated from PBMCs derived from an HIV-1-seronegative individual with HLA-B*52:01, HLA-B*51:01, or both were cultured. After the cells had been incubated with the desired HIV-1 clones for 4 h at 37°C, they were washed three times with RPMI 1640-10% FCS medium. The HIV-1-infected CD4$^+$ T cells were then cocultured with Pol283-8-specific CTL clones. From day 3 to day 7 postinfection, culture supernatants were collected and the concentration of p24 antigen (Ag) in them was measured by use of an enzyme-linked immunosorbent assay kit (HIV-1 p24 Ag ELISA kit; ZeptoMetrix).

**HLA stabilization assay with RMA-S cells expressing HLA-B*52:01 or HLA-B*51:01.** The peptide-binding activity of HLA-B*52:01 or HLA-B*51:01 was assessed by performing an HLA stabilization assay with RMA-S cells expressing HLA-B*52:01 (RMA-S-B*52:01) or HLA-B*51:01 (RMA-S-B*51:01) as described previously (33). Briefly, RMA-S-B*51:01 and RMA-S-B*52:01 cells were cultured at 26°C for 16 to 24 h. The cells ($2 \times 10^5$) in 50 μl of RPMI 1640 supplemented with 5% FCS (RPMI–5% FCS) were incubated at 26°C for 3 h with 50 μl of a solution of peptides at $10^{-3}$ to $10^{-7}$ M and then at 37°C for 3 h. After having been washed with RPMI–5% FCS, the cells were incubated for 30 min on ice with an appropriate dilution of TP25.99 MAb. After two washings with RPMI–5% FCS, they were incubated for 30 min on ice with an appropriate dilution of fluorescein isothiocyanate (FITC)-conjugated anti-mouse Ig antibodies. Finally, the cells were washed three times with RPMI–5% FCS and the fluorescence intensity of the cells was measured by the FACS-Cant II. Relative mean fluorescence intensity (MFI) was calculated by subtracting the MFI of cells not peptide pulsed from that of the peptide-pulsed ones.

**Sequencing of plasma RNA.** Viral RNA was extracted from the plasma of chronically HIV-1-infected Japanese individuals by using a QIAamp